MKS (SI-units) ⇔ CGS

- See pages 107-109 in "Van der Waals Forces" by Adrian Parsegian for full overview of conversion
- First example: Coulomb forces

in SI units	CGS units
Force $= \frac{q_1 q_2}{4\pi\varepsilon_0 r^2}$ N, q_1, q_2 in coulombs C, r in meters, $\varepsilon_0 = 8.85 \times 10^{-12}$ C^2 N^{-1} m^{-2} or $(1/4\pi\varepsilon_0) = 8.992 \times 10^9$ N m^2/C^2;	Force $= \frac{q_1 q_2}{r^2}$ dyn, q_1, q_2 in statcoulombs, r in centimeters.

- Second example: Poisson equation

$$\nabla \cdot (\varepsilon \mathbf{E}) = \rho_{\text{free}}/\varepsilon_0, \qquad \nabla \cdot (\varepsilon \mathbf{E}) = 4\pi\rho_{\text{free}}.$$

- Other conversion please see text book by A. Parsegian

http://www.damtp.cam.ac.uk/user/gold/teaching_biophysicsIII.html

Optical Trapping

- Why optical traps?
- How to build an optical trap?
- How does optical trapping work?
- Calibration of optical traps

http://www.damtp.cam.ac.uk/user/gold/teaching_biophysicsIII.html

Measurements of molecular forces

We discussed already that the thermal energy at room temperature is equivalent to
~10^{-21} J ⇔ ~25 meV ⇔ ~4 pNnm.

Polymers like DNA or other macromolecules in solvents are constantly exposed to the bombardment of the surrounding molecules or atoms.

One very nice example is the entropic stiffness of a polymer chain. We discussed this earlier in the course briefly as freely jointed chain in the section on fluctuation induced forces. This means that living organisms need to work in noisy environments where many forces are on similar order.

The value of 4 pNnm also gives us already an indication what kind of capabilities any technique would need to assess processes on this molecular scale.

In essence, we would like to be able to measure forces in the range of 10^{-12} Newton or even lower, and if possible with (sub-)nanometre spatial resolution.

There are three complementary single-molecule techniques that are widely used an lead to a revolution in biological physics since the 1990s.

Starting with ***optical tweezers***, we will learn how they are experimentally implemented and for which kind of experiments both in soft matter and biological physics they can be used. Then we will discuss ***magnetic tweezers*** and their use to twist DNA. Finally we will look into the ***atomic force microscope*** and its use for protein unfolding studies.

http://www.damtp.cam.ac.uk/user/gold/teaching_biophysicsIII.html

Optical Tweezers: Photonic Forces

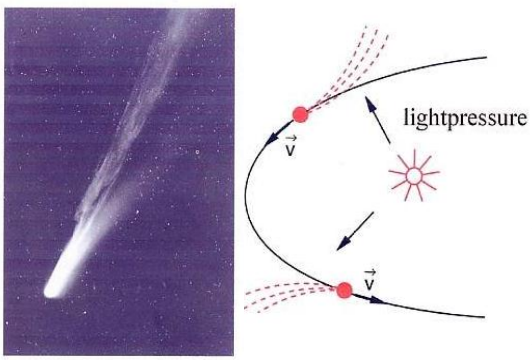

Photons carry momentum p depending on their wavelength λ

$$|\vec{p}| = \frac{h}{\lambda}$$

Where h is Planck's constant. This can be observed by the two tails of comets. One containing the heavier particles following the path of the comet and a second tail containing lighter atoms and molecules. From the observation of bent tails of comets, one can conclude that photons can interact with atoms/particles and transfer momentum.

One of the first quantitative explanations can be found in a publication from 1909 by Peter Debye. This is remarkable as the fundamental principles for optical tweezers are already laid out in the early days of quantum mechanics when the discovery that photons in fact carry momentum was just being discovered. On should also remember in this context that Einstein got the Nobel prize for the photoelectric effect - in 1921.

http://www.damtp.cam.ac.uk/user/gold/teaching_biophysicsIII.html

*Historical Note on Photonic Forces **

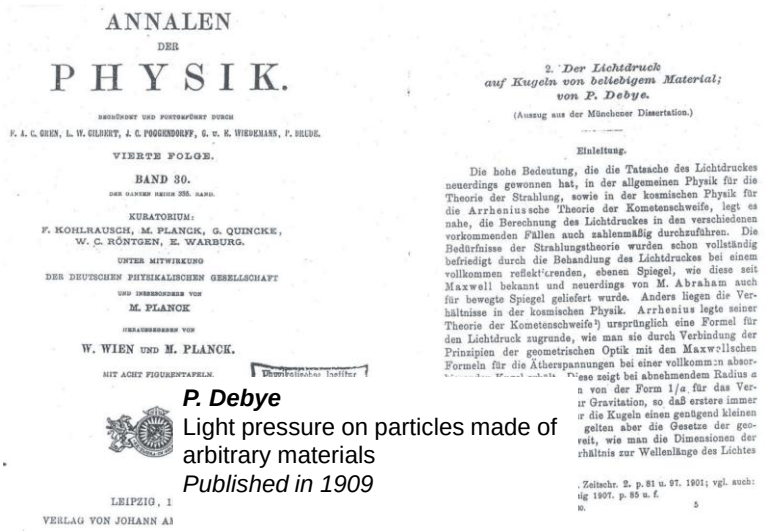

ANNALEN
DER
PHYSIK.

BEGRÜNDET UND FORTGEFÜHRT DURCH
F. A. C. GREN, L. W. GILBERT, J. C. POGGENDORFF, G. u. H. WIEDEMANN, P. DRUDE.

VIERTE FOLGE.

BAND 30.

DER GANZEN REIHE 325. BAND.

KURATORIUM:
F. KOHLRAUSCH, M. PLANCK, G. QUINCKE,
W. C. RÖNTGEN, E. WARBURG.

UNTER MITWIRKUNG
DER DEUTSCHEN PHYSIKALISCHEN GESELLSCHAFT
UND INSBESONDERE VON
M. PLANCK

HERAUSGEGEBEN VON
W. WIEN UND M. PLANCK.

MIT ACHT FIGURENTAFELN.

LEIPZIG, 1
VERLAG VON JOHANN A

2. *Der Lichtdruck auf Kugeln von beliebigem Material;*
von P. Debye.

(Auszug aus der Münchener Dissertation.)

Einleitung.

Die hohe Bedeutung, die die Tatsache des Lichtdruckes neuerdings gewonnen hat, in der allgemeinen Physik für die Theorie der Strahlung, sowie in der kosmischen Physik für die Arrheniussche Theorie der Kometenschweife, legt es nahe, die Berechnung des Lichtdruckes in den verschiedenen vorkommenden Fällen auch zahlenmäßig durchzuführen. Die Bedürfnisse der Strahlungstheorie wurden schon vollständig befriedigt durch die Behandlung des Lichtdruckes bei einem vollkommen reflektierenden, ebenen Spiegel, wie diese seit Maxwell bekannt und neuerdings von M. Abraham auch für bewegte Spiegel geliefert wurde. Anders liegen die Verhältnisse in der kosmischen Physik. Arrhenius legte seiner Theorie der Kometenschweife[1]) ursprünglich eine Formel für den Lichtdruck zugrunde, wie man sie durch Verbindung der Prinzipien der geometrischen Optik mit den Maxwellschen Formeln für die Ätherspannungen bei einer vollkommen absor-

ese zeigt bei abnehmendem Radius a
n von der Form $1/a$ für das Ver-
ir Gravitation, so daß erstere immer
ir die Kugeln einen genügend kleinen
gelten aber die Gesetze der geo-
reit, wie man die Dimensionen der
rhältnis zur Wellenlänge des Lichtes

, Zeitschr. 2. p. 81 u. 97. 1901; vgl. auch:
ig 1907. p. 85 u. f.
0. 5

P. Debye
Light pressure on particles made of arbitrary materials
Published in 1909

http://www.damtp.cam.ac.uk/user/gold/teaching_biophysicsIII.html

Estimating Photonic Forces

From the observations on comets one can deduce that photons carry momentum which can be transferred to atoms and molecules. To get a rough idea about the magnitude of the forces we can do a quick calculation. Assuming that photons are reflected by a perfect mirror, we can write down the light pressure exerted on the mirror. Let's define the intensity I as the power P per area A on the mirror

$$I = \frac{P}{A}$$

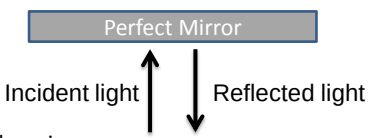

We can then write down the light pressure on the mirror p_r

$$p_r = 2\frac{I}{c}$$

where c is the speed of light. The factor of takes account of the fact that the light is reflected.

Assuming that our light source (laser) has an output power of P=500 mW we can estimate the force on the mirror F_r as

$$F_r = p_r A = 2\frac{P}{c} \approx 3.5\ \text{nN}$$

This is more than three orders of magnitude larger when compared to forces in the range of 10^{-12}N we want to measure. It is even more important to note that the gravitational force on a bacterium is in the range of 10 fN.

http://www.damtp.cam.ac.uk/user/gold/teaching_biophysicsIII.html

Optical Tweezers in Action

Before we discuss in detail how optical tweezers can be build and used, perhaps we can already look at a nice demonstration of the strong effects that light can have on single bacterial cells.

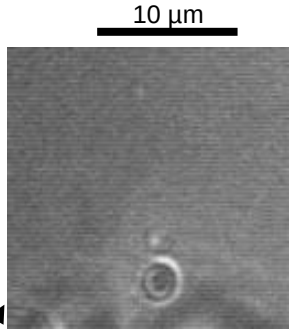

In the movie an infrared laser beam at a wavelength of 1064 nm is focussed into a diffraction limited spot with diameter of roughly 1 micron. In this experiment the power of the laser is 500 mW.

Here comes bacterium

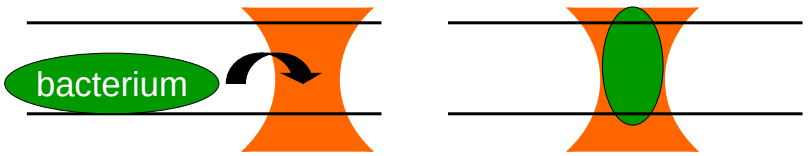

http://www.damtp.cam.ac.uk/user/gold/teaching_biophysicsIII.html

Optical Trapping in the Ray Optics Regime

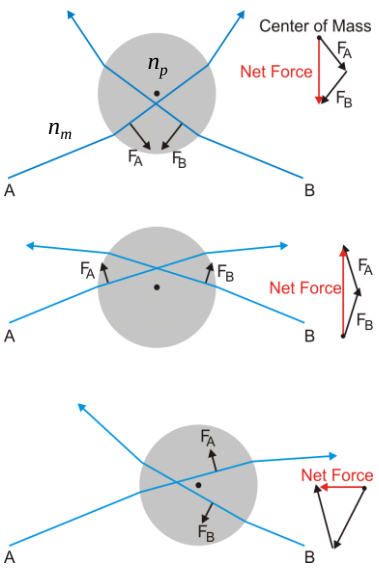

One straightforward approach to understand optical trapping can be discussed in the context of ray optics.

Assuming that the particle held in the laser focus is much larger than the wavelength of light, we can avoid Gaussian optics but simply use Snellius' law to understand the acting forces.

Upon hitting the interface between particle and surrounding medium the light is refracted at the interface. For trapping, the refractive index n_m of the medium should be lower than n_P of the particle. The change in direction of the ray leads to a change in momentum of the photons and thus a momentum acting on the particle. Depending on the initial position of the particle relative to the focal spot (indicated a black spot) the net force always pulls the particle back towards the focal point. This establishes a stable three-dimensional trapping, ***if*** these restoring forces are larger than the thermal forces and the scattering force (light pressure).The latter is neglected in this simple example, obviously.

http://www.damtp.cam.ac.uk/user/gold/teaching_biophysicsIII.html

Optical Tweezers: Schematic Setup 1

(Neuman 2004)

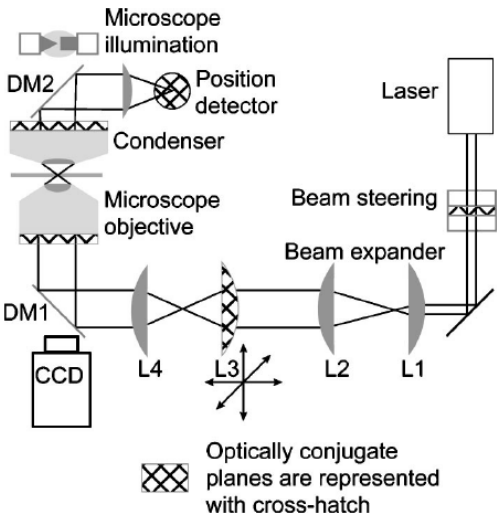

There is a wide range of possible experimental configurations for optical tweezers (OT).
In essence an OT setup needs a tightly focussed laser beam, usually achieved by focussing the beam through a microscope objective with high numerical aperture NA>1. For an optimal quality of the imaging, all elements should be adapted, apertures etc. This is achieved by introducing optically conjugated planes which are shown in the figure by the cross-hatched planes. If planes are optically conjugated it means that objects are in focus in all these plans at the same time.
In the example on the left, two microscope objectives are used. One for creating the trap and the second one for illumination and detection of the motion of the particle in the optical trap.

http://www.damtp.cam.ac.uk/user/gold/teaching_biophysicsIII.html

Reminder: Numerical Aperture

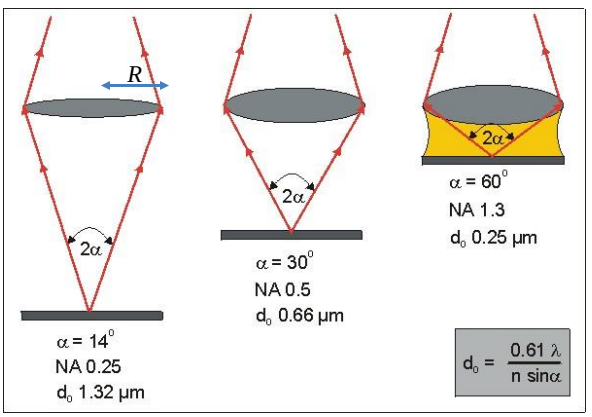

Numerical aperture determines resolution d_0 of the objective This is the minimal distance when two objects can be distinguished

Numerical aperture (NA) is defined as $NA = n \sin(\alpha)$, where n is the refractive index of the medium and α the opening angle of the objective lens.

The factor of 0.61 due to diffraction at round aperture which leads to the so called Airy disc that has minima at $0.61\lambda/R$, $1.116\ \lambda/R$, $1.619\ \lambda/R$, … with λ the wavelength and R the radius of the objective lens. The solutions of a plane wave incident on a round aperture leads to an intensity distribution described by Bessel functions of the first kind with poles at the positions given above. The resolution (for distinguishing objects) of any microscope is limited by the wavelength and the diffraction pattern of the lens.

http://www.damtp.cam.ac.uk/user/gold/teaching_biophysicsIII.html

Optical Tweezers: Position Detection in Reflection

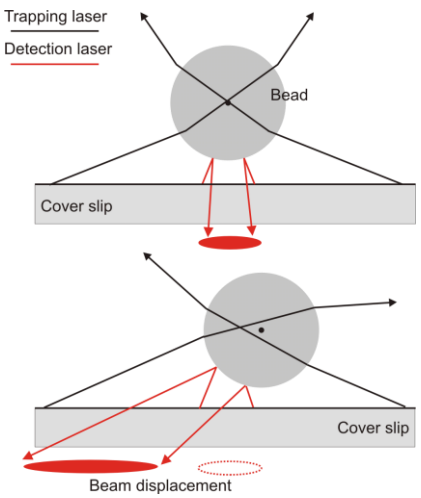

We will discuss two different strategies for the measurement of positions of a particle in an optical trap. Both methods we are discussing are extremely relevant for all techniques discussed in the lecture and are widely used in the tracking of single particles or molecules.

On the left, the detection of the position using a second laser beam, that is reflected off the particle is depicted. This is also the method of choice employed in the atomic force microscope. In general this technique allows for resolution down to 0.01nm and below. It is important to note here, that spatial resolution in particle tracking is NOT limited by the resolution determined by the NA of the used objective. The NA only determines at what distance two particles can be distinguished. This is important to remember, especially when modern developments like STED (stimulated emission depletion microscopy) are discussed which can overcome the limitations by NA.

http://www.damtp.cam.ac.uk/user/gold/teaching_biophysicsIII.html

Optical Tweezers: Quadrant Photodetectors

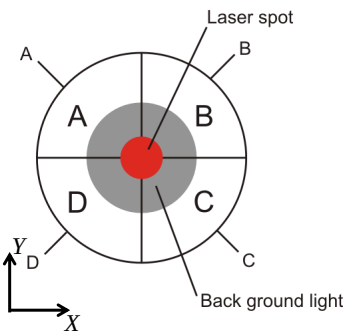

X position

$$X = \frac{(A+D)-(B+C)}{A+B+C+D}$$

Y position

$$Y = \frac{(A+B)-(C+D)}{A+B+C+D}$$

In order to detect the position of the red laser beam and thus determine the position of the trapped particle, one can use quadrant photodetectors . This approach is ubiquitous in experimental systems.

Four independent photodiodes (A,B,C,D) are combined into a single quadrant photodetector. Each element has its on amplifying circuit converting the incoming photons into a voltage A,B,C,D. The relative position of the laser beam can then be simply determined by comparing the incident power $C+D$ on two of the sectors $A+B$ with the two opposite ones $C+D$, while dividing by the total incident laser power.

Position measurements can be taken every 10^{-6}s and below. Most applications in soft and biological physics it is not necessary to go beyond due to the low Reynolds number environment.

Calibration of the detector response is necessary. One method to do this is the use of the powerspectrum of the optical trap that we will discuss next. Detection of sub-nm movements is possible. Obvious limitations of the resolution are related to electronic noise of detector, light level, background light, and size of laser spot on detector.

Video Based Particle Tracking

(Otto 2010)

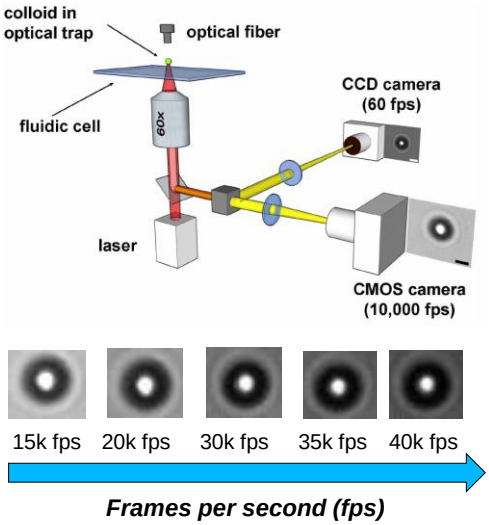

An alternative to quadrant photodetectors (QPDs) is using video cameras. There are several advantages with this approach, namely the possibility to follow several particles in parallel, easier calibration of the position information and reduction of drift (1/f-noise source) or electrical interference.

With an intense light source illuminating the sample, a fast camera is mounted behind the tube lens of the imaging microscope objective and the video recorded. Modern digital cameras can reach frame rates of 10,000 or more per second. The stream of images is captured by a computer for analysis of the position of the particles in the field of view. It is also possible to analyse the data on the fly in real time, removing the need to store GBs of video data and rather just saving two numbers for the x,y,z position of the particles in the image.

http://www.damtp.cam.ac.uk/user/gold/teaching_biophysicsIII.html

Cross-correlation position tracking

(Otto 2010)

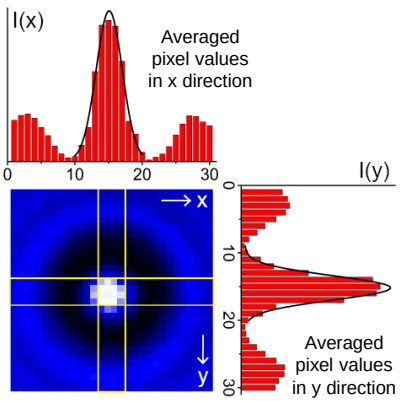

Region of interest

Yellow lines denote lines that are averaged to produce profiles on top and right. This reduces noise due to electronic noise in the electronics of the pixels.

Since the typical amplitude of the motion of a trapped colloid is of the order of tens of nanometres, and typically one pixel on a camera corresponds to a few hundred nm, position determination must be carried out with subpixel accuracy.

In particle tracking we use a number of assumptions to obtain a sub-pixel resolution: (i) the particles should be rotationally symmetric and produce a symmetric diffraction pattern on the camera that is (ii) constant over time.

For the determination of the particle position in the region of interest one can use a cross-correlation based tracking algorithm. Sub-pixel accuracy is achieved by calculating the cross-correlation of the mean intensity distribution with its reverse by applying the convolution theorem. The convolution theorem uses that the Fourier transforms of signals f and g is equal to the point wise product of each their Fourier transforms.

http://www.damtp.cam.ac.uk/user/gold/teaching_biophysicsIII.html

Sub Pixel Resolution with Video Tracking

(Otto 2010)

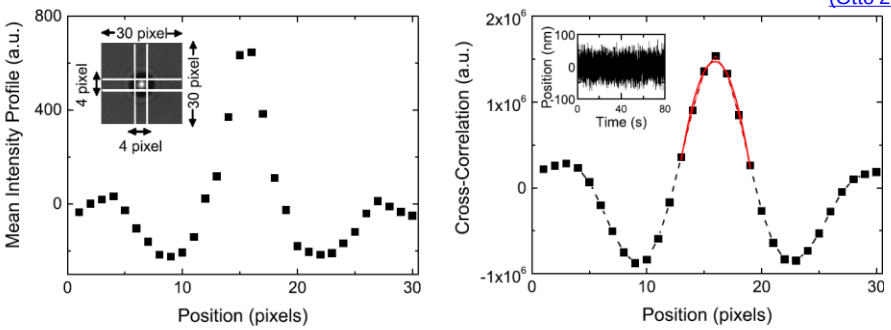

After calculation of the mean intensity profile along an 4×30px2 rectangular array of the 30×30px2 sub-ROI (see inset in (a)) , the intensity profile is depicted in *x*- and *y*- direction (a). Cross-talk between the directions is minimal, this is another advantage over QPD tracking. Part (b) shows 1-dimensional cross-correlation transformation and 2nd-order polynomial fit of ±3px around the maximum. The fit shows why we can achieve sub-pixel resolution with this technique. As we assume that the shape of the intensity profile is constant over time and the cross-correlation can be approximated by a simple polynomial, even with a fit of only seven points we achieve a resolution of a few nm in this case.
The inset in (b) shows a time trace for a colloid tracked for 80 s at 10,000 fps in real-time.

http://www.damtp.cam.ac.uk/user/gold/teaching_biophysicsIII.html

Resolving nm steps with video tracking

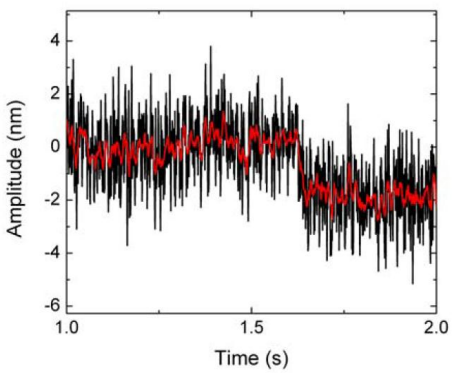

One can test the tracking routine by investigating the motion of of a surface attached colloidal particle that is moved in defined steps. In order to determine the resolution in the instantaneous position of a particle a 3.47 µm silica particle was adhered to the surface of a sample cell and a piezoelectric stage was moved in 2nm steps.
The plot on the left shows the change in the detected position signal of the particle following a 2 nm step of the piezoelectric stage. Analysis of the data reveals that our tracking algorithm can resolve step size with an accuracy of down to 0.2 nm. The red line is calculated using a moving, adjacent average filtering over 10 data points.

http://www.damtp.cam.ac.uk/user/gold/teaching_biophysicsIII.html

Brownian Motion of a Particle in an Optical Trap

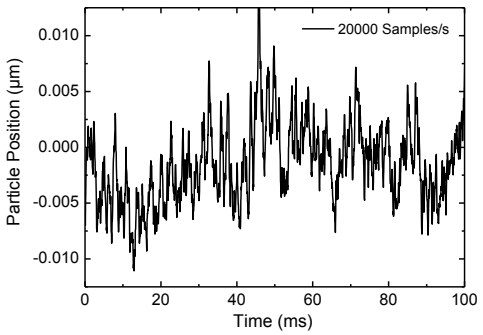

On the left, a example for the Brownian motion of a spherical particle in an optical trap is shown. The position was measured with a calibrated quadrant photo detector. The position-axis already shows the signal in micrometres. The conversion of the voltage output of the photo detector is usually achieved by moving a stuck particle with a calibrated piezoelectric stage in the nanometre range. This is raw data, without taking care about filtering, background corrections or other analysis methods.

We will now investigate how this type of data can be used to calibrate the forces acting in the optical trap. To first approximation we assume that the trap is harmonic for small deviations from the trap centre, i.e. the restoring force driving the particle back into the equilibrium position is proportional to distance. This is of course just Hooke's law $F=-\kappa\Delta x$, where κ is the trap stiffness in that direction and Δx the distance from the trap centre. In general, optical traps are not isotropic but have to be described with a two-dimensional matrix.

http://www.damtp.cam.ac.uk/user/gold/teaching_biophysicsIII.html

Calibration: Equipartition - Position Histograms

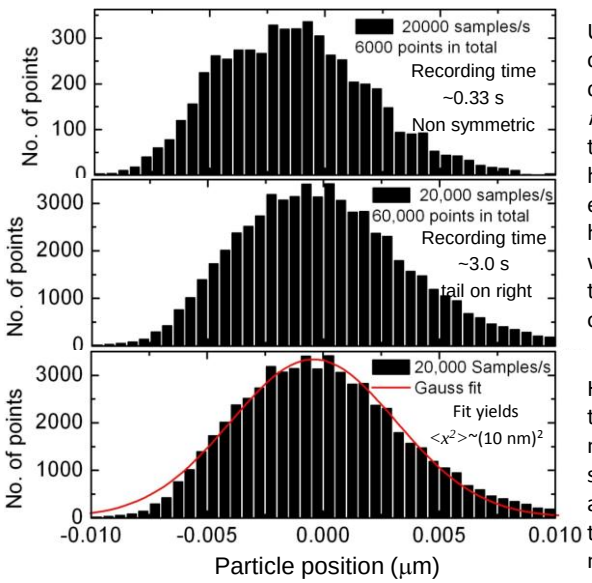

Expected variance for all cases: $\langle x^2\rangle$ ~(11 nm)²

Using the equipartition theorem we can extract information from the data to determine the trap stiffness κ of the optical trap. At constant temperature T, a particle in a harmonic potential has a thermal energy of $\frac{1}{2}k_BT$. Assuming an harmonic potential we can directly write down the expected width of the random particle positions in the optical trap to be

$$\langle x^2\rangle = k_B T/\kappa$$

However, in the case of a real data, there are complications with this method. The position histograms shown on the left are clearly asymmetric, depending on recording times and time resolution of measurements. This is due to other sources of error like 1/f-noise etc.

http://www.damtp.cam.ac.uk/user/gold/teaching_biophysicsIII.html

Calibration: Using Power Spectrum

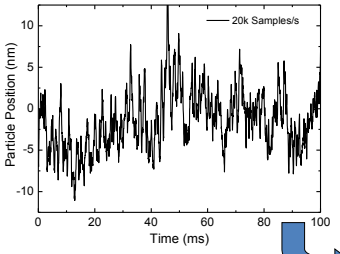

From the time dependent particle positions we calculate the power spectral density by Fourier transform of the positions into the frequency domain. With Parseval's theorem we can also conclude that the total power for both cases has to be the same.

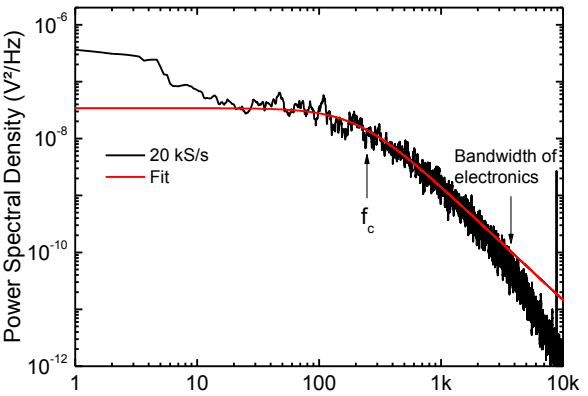

Fourier Transform: $H(f) = \int_{-\infty}^{\infty} h(t) e^{2\pi i f t} dt$

Total Power $= \int_{-\infty}^{\infty} |h(t)|^2 \, dt = \int_{-\infty}^{\infty} |H(f)|^2 \, df$

We use here not angular frequency but $f=\omega/2\pi$ since this removes prefactors of 2π. Here, we are interested in the one-sided power spectral density:

$P_h \equiv |H(f)|^2 + |H(-f)|^2 = 2|H(f)|^2$ if $H = H^*$

http://www.damtp.cam.ac.uk/user/gold/teaching_biophysicsIII.html

Power Spectra as a function of Laser Power

Otto (2008)

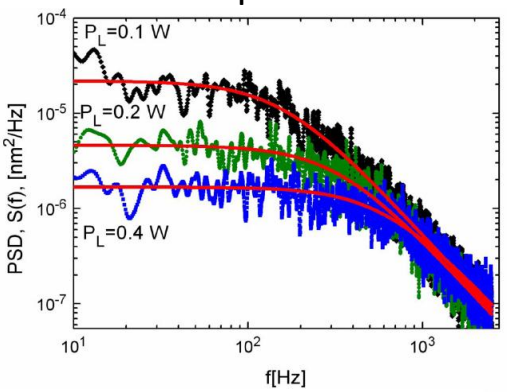

To first approximation we would expect that the trap stiffness depends linearly on the applied laser power. In practice this holds for most situations, as shown by the data below. Corrections due to heating are usually in the range of a few per cent or even less and do not show up at the low frequency range however can sometimes be observed at higher frequencies.

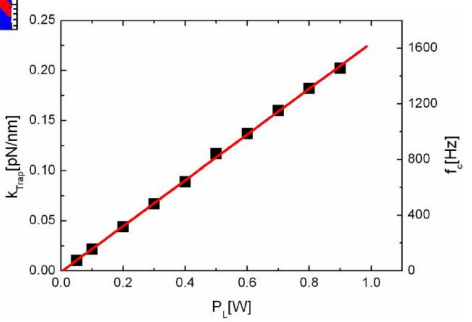

The trap stiffness should not be confused with the maximum force optical tweezers can exert. These are in the range of a few 10s of pN. Obviously force and position resolution critically depend on the stiffness. By tuning of the laser power one can easily choose the required stiffness. This allows for adaption to the forces that should be measured.

http://www.damtp.cam.ac.uk/user/gold/teaching_biophysicsIII.html

Test of Calibration of Optical Trap

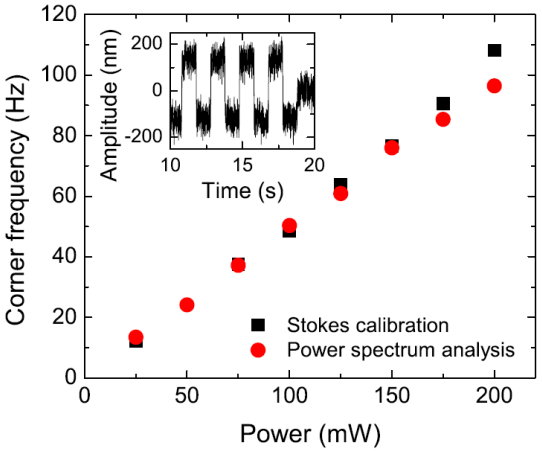

One staightforward check of the trap stiffness calibration is by using Stokes drag on the particle. By dragging a particle of known diameter through the liquid at known speed v we have force $F=\gamma v$. One has just to compare the measured force with the expected force. As in the trap calibration, the biggest uncertainties in these measurements are the particle diameter and the temperature of the liquid in the optical trap. Depending on the laser wavelength, it might heat the liquid. As the viscosity is temperature dependent this influences the drag coefficient of the particle and thus the Stokes drag.

Laser induced changes of the temperature around the particle can be detected with sensitive detection especially in the high frequency range of the powerspectra (see question sheet) where the particle is 'freely' diffusing in the optical trap.

http://www.damtp.cam.ac.uk/user/gold/teaching_biophysicsIII.html

*Influence of Bandwidth on Powerspectra **

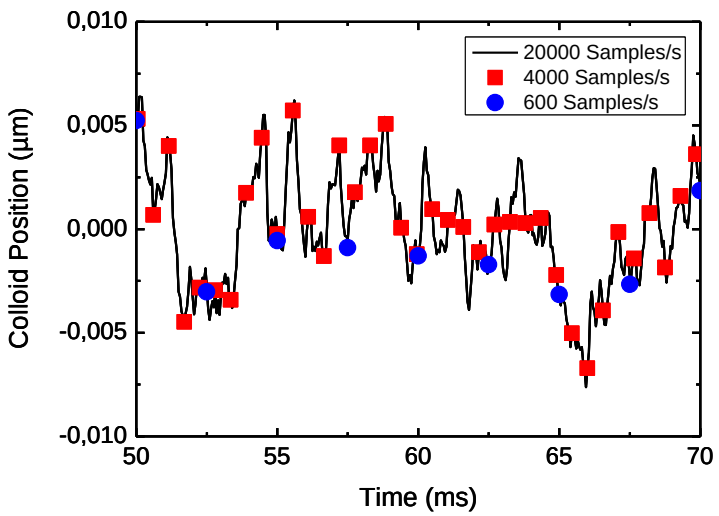

The bandwidth or number of samples/second of the optical trap system is crucial for an accurate determination of the trapping stiffness using the powerspectral analysis method. If the same signal is digitized with a range of different samples/s but with the same temporal resolution this has a profound influence on the powerspectrum.

Issues with REAL Data: Aliasing

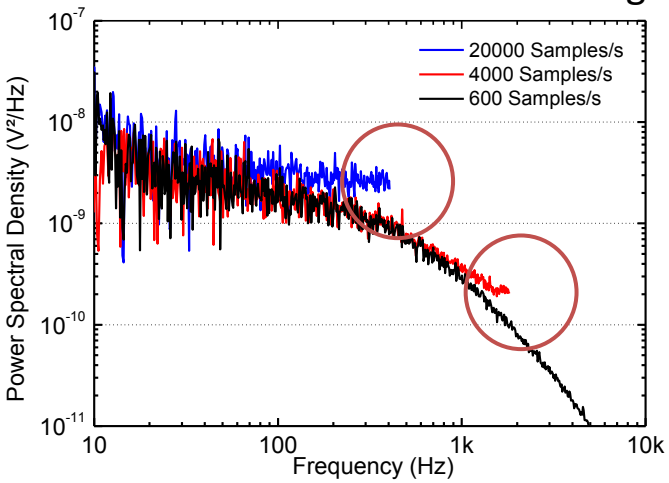

Sampling with the same temporal resolution but lower bandwidth leads to an increase of power in the low frequency part of the spectrum. This is the well known effect of aliasing, leading to so-called ghost frequencies in the spectrum. Obviously, this fundamentally changes the shape of the powerspectrum, rendering it useless for calibration.

http://www.damtp.cam.ac.uk/user/gold/teaching_biophysicsIII.html

Issues with REAL Data in Video Tracking

Video tracking produces aliasing since pixels are not exposed during the full time, since the camera electronics needs a finite amount of time to read the data from the pixel into the memory of the camera/computer.

A typical example is shown below for three different trapping laser powers imaged at 10,000 fps. The nominal shutter time would be Δt=100 μs, however the real time tempral resolution is Δt=95 μs which makes the real bandwidth is 5,263 Hz.

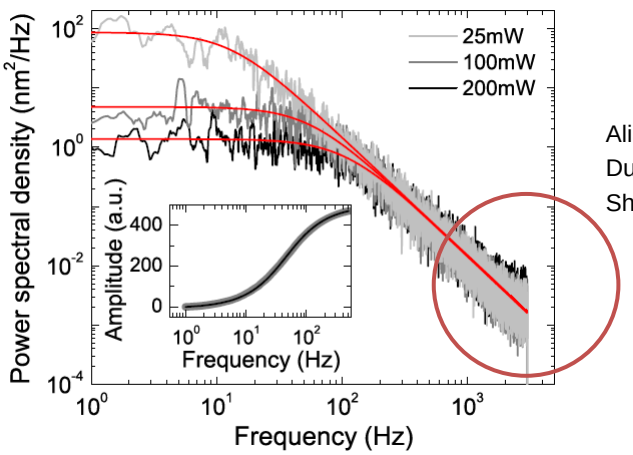

Aliasing
Due to camera
Shutter time

*REAL Data: 1/f noise and bandwidth **

To avoid problems with aliasing quadrant photo detector electronics have inbuilt low-pass filters which limit the bandwidth. This shows up as a faster drop in the powerspectrum at frequencies larger than the filter drop off. In the ideal case the recording bandwidth should be always at least 2 times higher than measurement bandwidth.

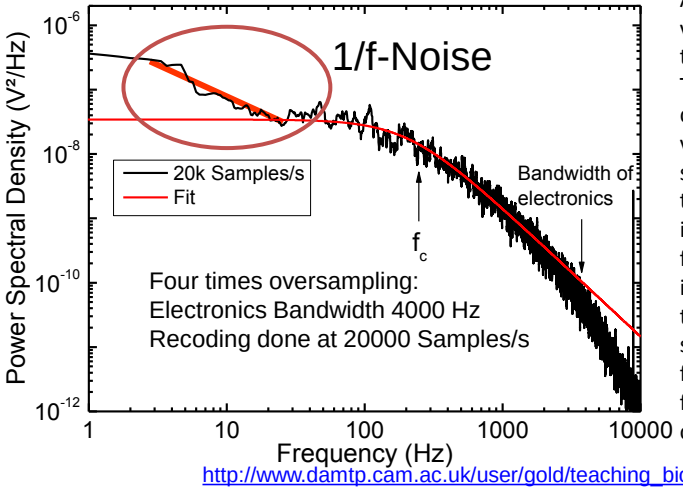

Another feature seen at very low frequencies is the so called 1/f noise. This can be due to thermal drift, mechanical vibrations or other noise sources interfering with the measurement. There is not one single source for this 1/f-noise however it severely limits the long term stability of the system and is the reason for equipartition often failing to predict the correct stiffness.

http://www.damtp.cam.ac.uk/user/gold/teaching_biophysicsIII.html

More possibilities for Optical Tweezers

Tetris with multi beam optical tweezers

http://www.youtube.com/watch?v=jCdnBmQZ6_s&feature=player_embedded

http://www.damtp.cam.ac.uk/user/gold/teaching_biophysicsIII.html

Optical Tweezers work in air and vacuum …

Water droplet trapped in air imaged at 2000 frames per second

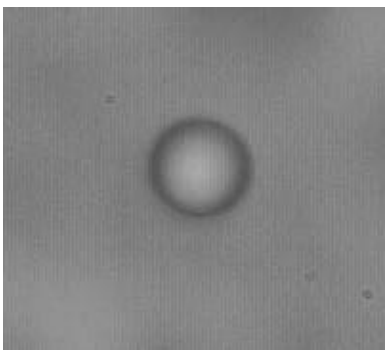

Padgett group Glasgow

http://www.damtp.cam.ac.uk/user/gold/teaching_biophysicsIII.html

Double Stranded DNA forms a Double Helix

Calladine & Drew Chapter 2 (1997)

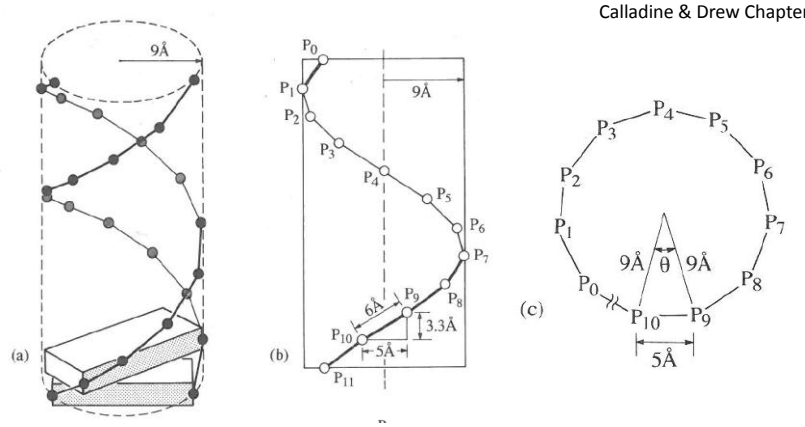

DNA is a co-polymer with a phosphate backbone and functional side-chains consisting of the four bases, Adenosine (A), Thymine (T), Guanine (G) and Cytosine (C). Hydrogen bonding (Watson-Crick) between the bases (A-T, G-C) holds the two backbone strands together. The formation of the double helix (shown here is the B-form) minimizes water between hydrophobic basepairs by twisting the basepair against each other. This is possible due to the flexibility of the backbone structure and its phosphate group. The phosphate group also leads to the negative charge of DNA in aqueous solution at pH>5.

http://www.damtp.cam.ac.uk/user/gold/teaching_biophysicsIII.html

Helix possible due to Rotating Bonds

Calladine & Drew, Chapter 2 (1997)

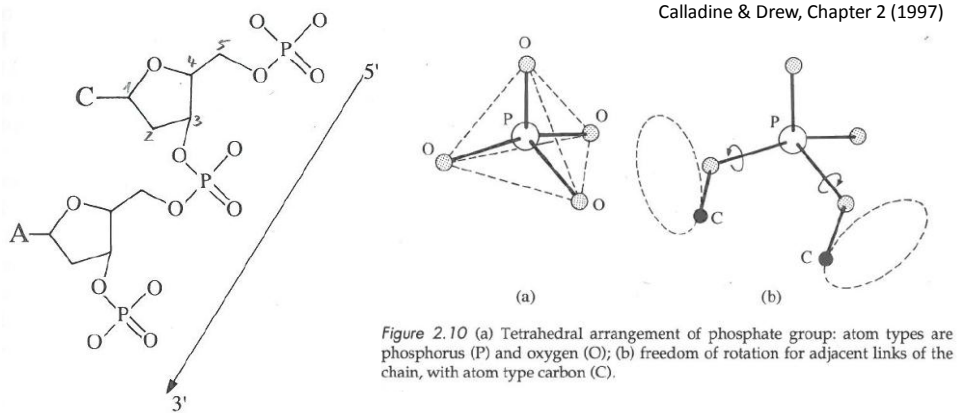

Figure 2.10 (a) Tetrahedral arrangement of phosphate group: atom types are phosphorus (P) and oxygen (O); (b) freedom of rotation for adjacent links of the chain, with atom type carbon (C).

The double helix is a consequence of the freedom of the C-atom to "swivel" around the P-O bond. This makes the DNA-backbone flexible to rotate and adapt its structure. It is also interesting to note that the backbone has a direction. As shown above, the C atoms in the sugar ring a labelled from 1-5. The phosphate group is either attached at the 5' or 3' end of the sugar and thus DNA ends a labeled as the 3' or 5'. In the double helix the strands are usually running anti-parallel. The flexibility of the backbone and in fact of the hydrogen bonding makes DNA a highly adaptable molecule depending on the conditions.

http://www.damtp.cam.ac.uk/user/gold/teaching_biophysicsIII.html

Some Forms of ds-DNA

Calladine & Drew Chapter 2 (1997)

DNA can be found not in just the standard B-double helix but also take different forms. There are many structural variants known which are usually labeled by a letter A, B, C, D, E, P, Z, … Most of these are right-handed double-helices, however as seen on the right, they can have different pitch, diameter and differences in the size of the major and minor grooves. Even the formation of a left handed helix is possible, as shown by the example for the Z-DNA. Since DNA structure was analysed by x-ray crystallography, the most prevalent forms (A,B) were discovered first as they can be easily crystallized. This illustrates that double-stranded DNA is a dynamic and adaptable building block of the living cell. It should also be clear that the different forms have distinctive mechanical properties which can be determined with optical tweezers.

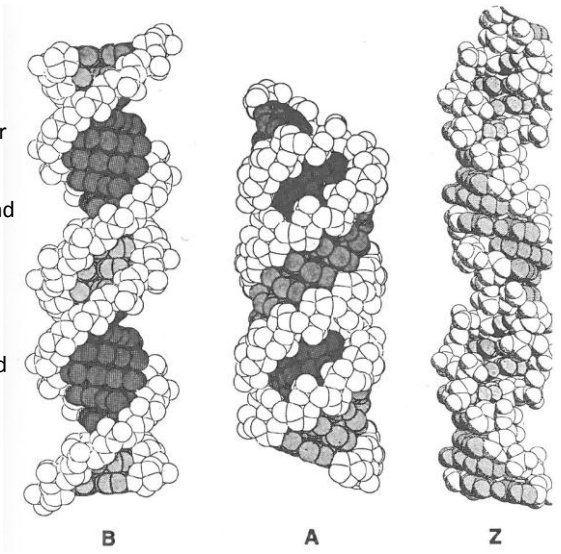

http://www.damtp.cam.ac.uk/user/gold/teaching_biophysicsIII.html

*dsDNA shows Intrinsic Curvature **

Calladine & Drew, Chapter 5 (1997)

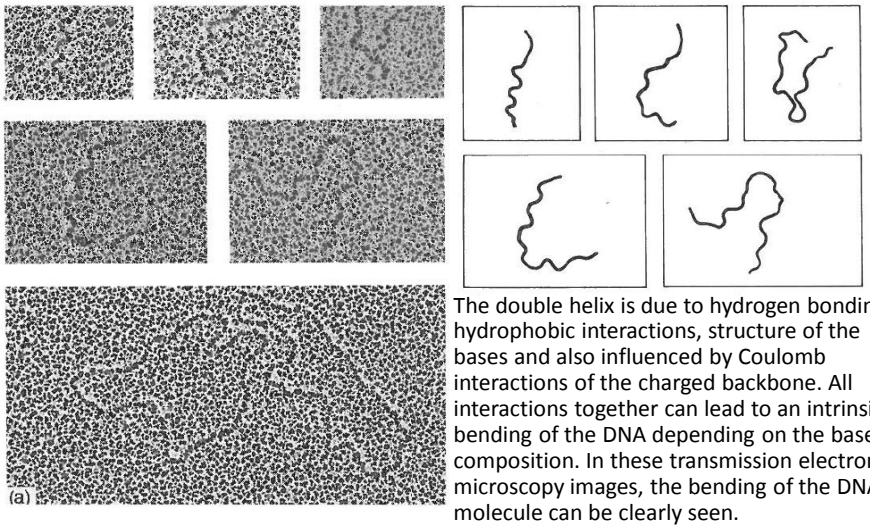

The double helix is due to hydrogen bonding, hydrophobic interactions, structure of the bases and also influenced by Coulomb interactions of the charged backbone. All interactions together can lead to an intrinsic bending of the DNA depending on the basepair composition. In these transmission electron microscopy images, the bending of the DNA molecule can be clearly seen.

These bends are implicated in playing a role in gene regulations and thus might play an important structural role in the functioning of cells, underlining again that DNA is not simply a B-form double helix.

http://www.damtp.cam.ac.uk/user/gold/teaching_biophysicsIII.html

Single-Stranded DNA (ssDNA)

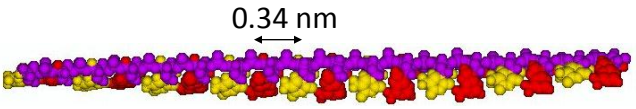

Single-stranded (ss)DNA is a copolymer consisting of phosphodiester backbone (purple), linked by single bonds and allowing to bind side chains or bases (red,yellow). The distance between the bases is 0.34 nm. ssDNA is not very often found freely in cells. In general hydrogen bonding between the bases will lead to formation of more complicated structures like hairpins or even more complex molecular complexes.

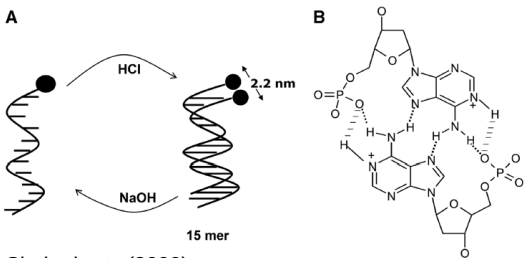

Chakraborty (2009)

Even ssDNA can have a helical form, depending on the exact base sequence, but it is freely rotatable due to the PO-C bonds. One specific molecule forming a helix is consisting of long stretches of A bases, which then, due to hydrophobic interactions giving rise to base-stacking, forms a compact single helix with an outer diameter of . It can even be found as a double-helix under acidic conditions.

http://www.damtp.cam.ac.uk/user/gold/teaching_biophysicsIII.html

Stretching a One Dimensional Chain

Phillips et al. , Chapter 8 (2009)

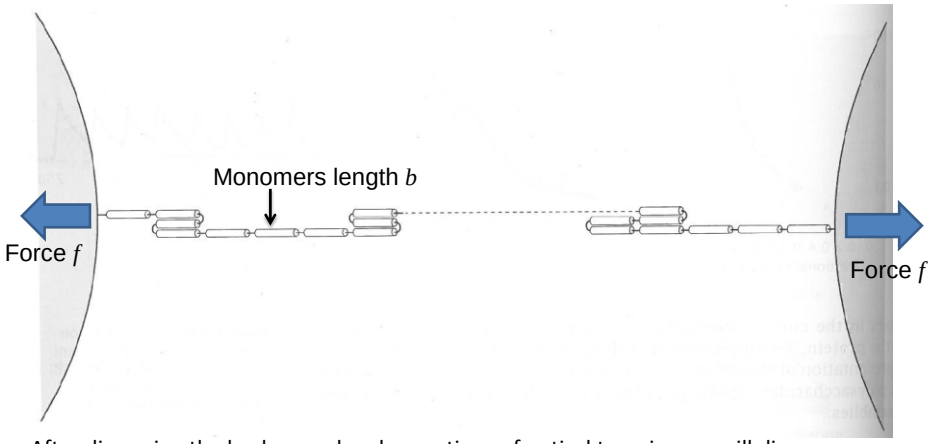

After discussing the background and operations of optical trapping we will discuss now the main use of these instruments in polymer and biolgical physics, namely the stretching of polymer chains. First we will discuss the ideal case with overlapping elements, no constraints and ideal bonds and later discuss more complex models like the worm-like chain already known from the Part II soft matter course (P. Cicuta).

http://www.damtp.cam.ac.uk/user/gold/teaching_biophysicsIII.html

Force Extensionof the 1D, 2D and 3D chains

Phillips et al. , Chapter 8 (2009)

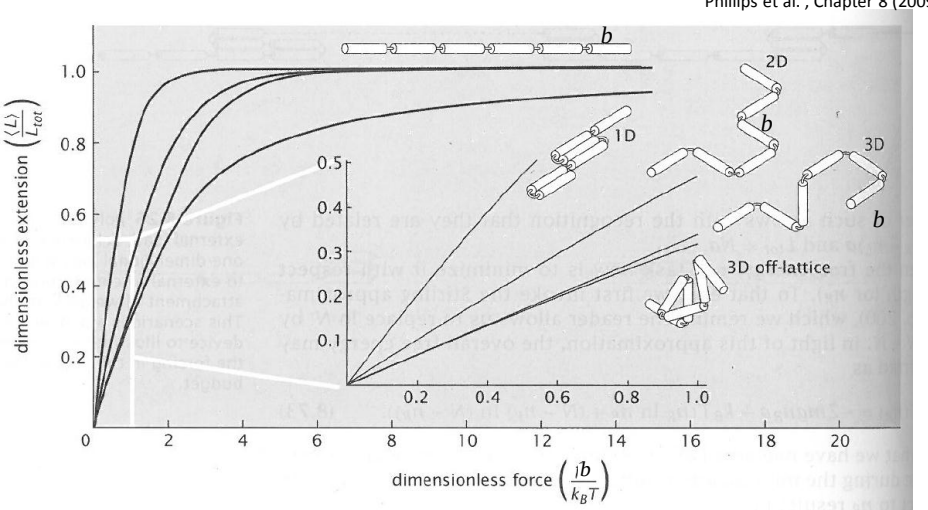

With the model we just developed and we can calculate the force extension or as shown here, the time averaged $<L>$ extension as a function of force, for 1D to 3D chains with extension normalized by $L_{tot}=Nb$ which is the contour length with N number of segments at constant temperature.

http://www.damtp.cam.ac.uk/user/gold/teaching_biophysicsIII.html

Blob Picture for Real Polymer Chains

Rubinstein, Colby, Chapter 3 (2005)

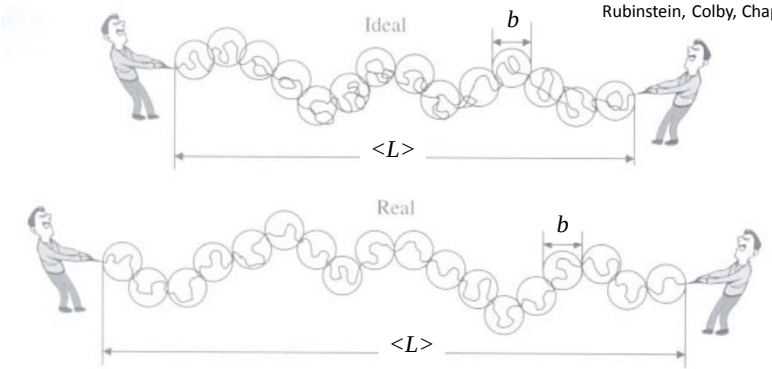

It is interesting to note that all real polymer chains can be made ideal if they are long enough. This can be understood by redefinition of the segment length to fulfil the condition $<R^2>=N'b'^2$. Here we introduce b or b' as the 'Kuhn'-segment length with $b=2p$. The Kuhn length is commonly used, however, we will use more often p which is the persistence length as defined in the worm-like chain that we will discuss now in more detail. The main difference between that follow Hooke's law and polymer chains is that, depending on the dimensionality and nature of the bonds, the force is a power law as a function of the extension.

http://www.damtp.cam.ac.uk/user/gold/teaching_biophysicsIII.html

Single-stranded DNA is an Extensible FJC

(Bustamante et al. Science 1996)

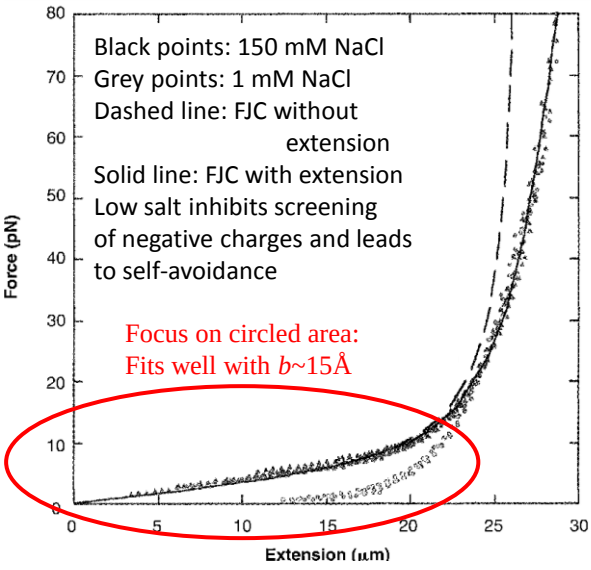

Force-extension measurements on ssDNA can be also performed with optical tweezers. The data can be easily fit with a model describing the freely-jointed chain (FJC, dashed line) at low forces, however at higher forces and long extensions the model significantly deviates and overestimates the results. This can be taken into account by making the length of the monomers force dependent $b(F)$, which leads to an almost perfect description of the data. Note that the charge of the DNA backbone and thus the Coulomb interactions significantly changes the behaviour at low salt concentrations as we will se later also for dsDNA.

http://www.damtp.cam.ac.uk/user/gold/teaching_biophysicsIII.html

Worm-like chain model (WLC)

Nelson, Chapter 9 (2006)

We discussed the freely-jointed chain as a good description of single-stranded DNA. However now we will try to understand the more complicated case of double-stranded DNA. The complications arise from the helical structure of the molecule as we discussed before. But the system contains so many atoms that calculations of the mechanical properties from first principles is too computationally expensive. So we will have to use some major simplifications that nevertheless can produce predictions that will be experimentally accessible. The idea is to describe dsDNA as a continuous rod, comparable to a beam of steel. We will test three different distortions of the dsDNA molecule, bending, stretching and twisting. These can be described within the following coordinate system.

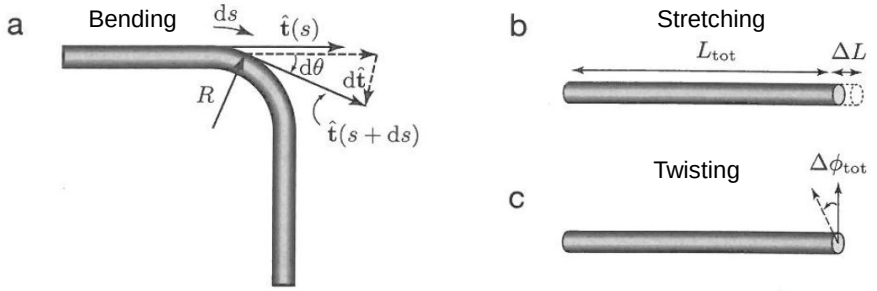

http://www.damtp.cam.ac.uk/user/gold/teaching_biophysicsIII.html

Four Parameters Characterize dsDNA (WLC)

Nelson, Chapter 9 (2006)

We will use three quantities to describe the dsDNA beam. First we will use the scalar stretch *u(s)* which measures the fractional change in length of the segment, where *s* denotes the position along the DNA. The bend deformation $\beta(s)$ describes the change of the tangent vector *t*, when the molecule is distorted (a). $\beta(s)$ is a vector with dimension [1/L]. Finally we will use the twist density $\omega(s)$ which describes the torsional deformation of the molecule. With this we describe the change of the angle along the length of the dsDNA. Obviously, *u(s)*, $\beta(s)$ and $\omega(s)$ are local quantities so we will have to integrate over the total unstretched length of the molecule to obtain the change energy:

$$dE = \frac{1}{2} k_B T \left[A\beta^2 + Bu^2 + C\omega^2 + 2Du\omega \right] ds$$

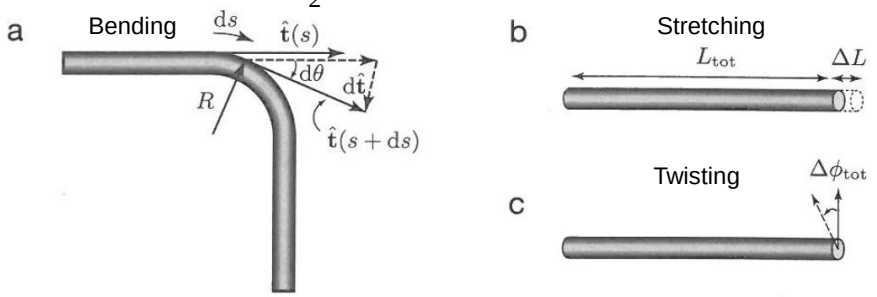

http://www.damtp.cam.ac.uk/user/gold/teaching_biophysicsIII.html

Making a bend in DNA

Nelson, Chapter 9 (2006)

$$dE = \frac{1}{2} k_B T \left[A\beta^2 + Bu^2 + C\omega^2 + 2Du\omega \right] ds$$

To calculate the change in energy dE, we introduce now four parameters A,B,C and D. All four parameters can be experimentally determined. The obvious interpretation of A is the persistence length of the molecule. C is the twist persistence length that, as we will see in the next section, describes the buckling transition of the DNA molecule. Bk_BT and Dk_BT are the stretch stiffness and twist-stretch coupling. In the following discussion we will assume that – at the forces we are working at – $B\&D=0$. fractional change in length of the segment, where s denotes the position along the DNA. For the case of single-stranded DNA we can also set $C=0$ as the molecule can freely rotate around its axis. Thus twisting will not lead to any distortions in the molecule.

Thus, in the simplest case we will treat DNA as an inextensible rod and, assuming that we do not twist the molecule, we can calculate the energy needed for making bending the molecule

$$E = \frac{1}{2} k_B T \int_0^L A\beta^2 ds$$

which is known as the simplified elastic rod model. (This is also named Kratky-Porod model.) With this equation we can now easily calculate the energy needed to bend the molecule by 90deg. This can be used to estimate the energy needed to make a plectoneme or supercoil into the DNA molecule (see question sheet). It is important to note that despite the major simplifications, the worm-like chain model works extremely well.

http://www.damtp.cam.ac.uk/user/gold/teaching_biophysicsIII.html

Video pulling single chains

video

http://www.damtp.cam.ac.uk/user/gold/teaching_biophysicsIII.html

Twisting DNA using Magnetic Tweezers

(Phillips 2009)

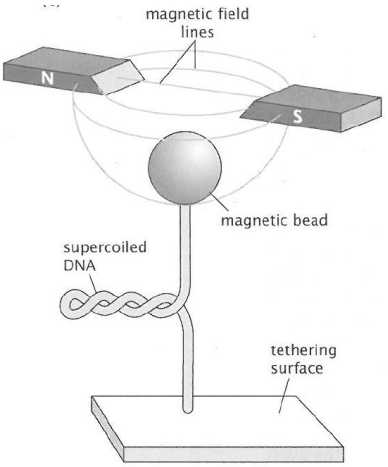

Until now we discussed optical tweezers as one of the methods that allows to interrogate the physics of single molecules. Although they revolutionized single molecule biophysics, optical tweezers have obvious limitations. By construction, optical tweezers are defining the position of a particle, this is also known as **position clamping**. OTs can move dielectric particles around but they cannot exert torque onto a molecule. However, twisting a molecule is a very important process in cells as protein motors walking along the double-helix of the DNA molecule induce significant torque. Thus we require a technique that enables to **exert torque** on the molecule. One obvious choice for a technique is the magnetic fields. The idea of magnetic tweezes is as simple as elegant. A gradient in a magnetic field leads to a force on a magnetic particle with magnetic moment μ_r . This leads to a force towards the magnets, while the direction of the magnetic moment allows for rotating of the particle with a rotation of the magnets. It is also important to notice that magnetic tweezers are **force clamps**, in contrast to OT which are position clamps.

http://www.damtp.cam.ac.uk/user/gold/teaching_biophysicsIII.html

*Supercoiling is important for the cell **

Massive supercoiling is generated by DNA motors,
e.g. during transcription and replication

Liu & Wang, PNAS 1987

Biological background: in the cell specialized enzymes have to regulate supercoiling to enable replication of DNA (see movie). During the replication of DNA the replication forc (composed of several enyzmes) moves through the DNA inducing negative and positive supercoils. These have to be removed (in a controlled way) by specialized enzymes known as topoisomerases, gyrases. Supercoiling can also be induced by many other DNA binding enzymes and studied by magnetic tweezers.

http://www.damtp.cam.ac.uk/user/gold/teaching_biophysicsIII.html

Magnetization of the beads is anisotropic

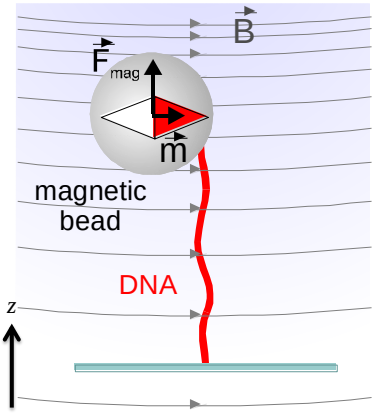

It is essential to have magnetic particles with a finite magnetic moment μ_r. This is acheived by using many small ferromagnetic nanoparticles that are inserted into a polymeric colloidal particle.
The energy E of the magnetic dipole in the magnetic field B is then:

$$E = -\vec{\mu}_r \cdot \vec{B}$$

and thus we can calculate the force in z direction

$$\frac{dE}{dz} = -\frac{d}{dz}\left(\vec{\mu}_r \cdot \vec{B}\right)_z$$

Obviously, the particle orients itself along a preferred axis determined by the outside field. With typical particles with diameters of a few microns, one can create pN forces and thus rotate the particle and any attached (bio)molecules. As mentioned before, this **allows twisting/supercoiling of DNA molecules** by rotating the magnets.

http://www.damtp.cam.ac.uk/user/gold/teaching_biophysicsIII.html

Schematic of Magnetic Tweezers

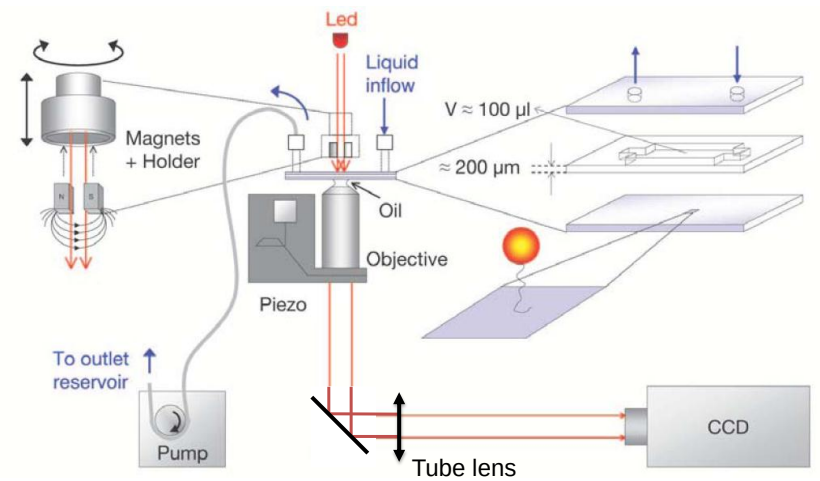

Magnetic tweezers are basically an inverted microscope, with a light source (LED). Two permanent magnets are mounted in a rotatable holder, the gap determines the gradient and thus the force. The force can be controlled by moving the magnet holder up or down with respect to the molecule attached (tehtered) to a microscope slide and the magnetic particle. This is usually achieved by employing receptor-ligand interaction with proteins extracted from cells.

http://www.damtp.cam.ac.uk/user/gold/teaching_biophysicsIII.html

*Magnetic Tweezers in the Lab **

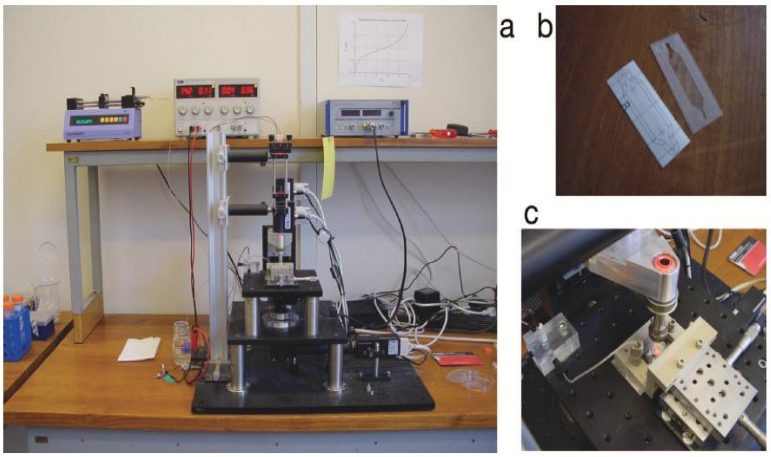

Magnetic tweezers can be build in very compact form. They are amazingly simple if one considers the exceptionally high resolution of forces. They can detect forces of less than 10 fN. However, the name tweezers is a bit misleading as strictly speaking they are only applying a force and do not define a position.

http://www.damtp.cam.ac.uk/user/gold/teaching_biophysicsIII.html

*Magnetic Tweezers Position Detection in Z **

Gosse, Croquette 2002

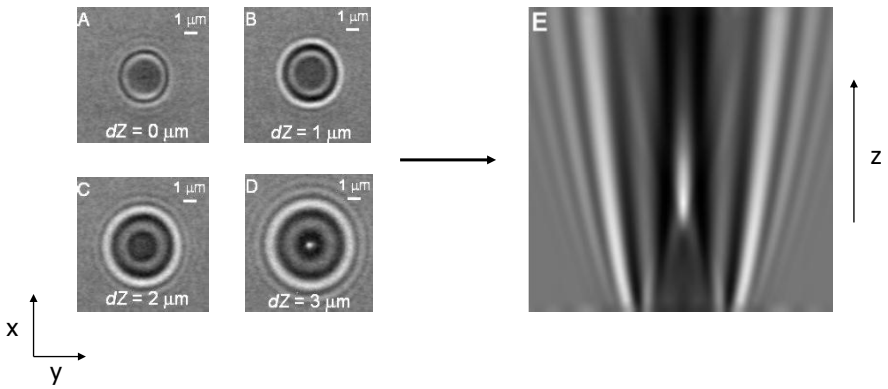

One of the challenges in magnetic tweezers is the detection of the distance between the colloidal particle and the surface of the sample cell. Here, the diffraction pattern of the particle on the camera can be used to determine the relative position of the particle to a pre-recorded look-up table shown in part E of the above figure. In practice, two particles are used to measure the length of the molecules. One particle is stuck to the glass indicating where the molecule is tethered to at one end while the other end is labeled with the second colloidal particle.

http://www.damtp.cam.ac.uk/user/gold/teaching_biophysicsIII.html

Magnetic Tweezers Force Measurements

(Seidel 2005)

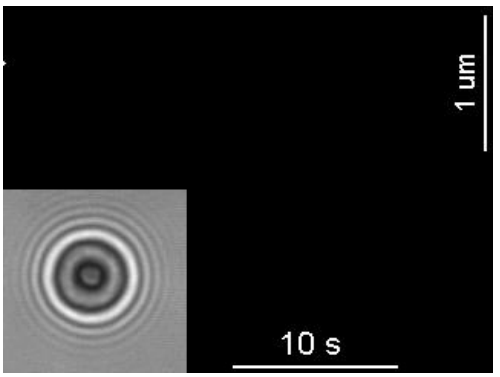

The movie demonstrate the functions of magnetic tweezers. The lower left shows the video microscopy image of a magnetic particle connected to the surface by a single dsDNA molecule. The magnets are placed at three different heights above the sample and thus the DNA molecule is stretched by applying three different forces. Obviously, as the DNA molecule is relaxed, its stiffness decreases. This is indicated by the increase of the Brownian fluctuations of the particle, which directly reflect the change in stiffness of the DNA molecule and the higher applied forces.

http://www.damtp.cam.ac.uk/user/gold/teaching_biophysicsIII.html

Magnetic Tweezers Calibration: Forces in x,y

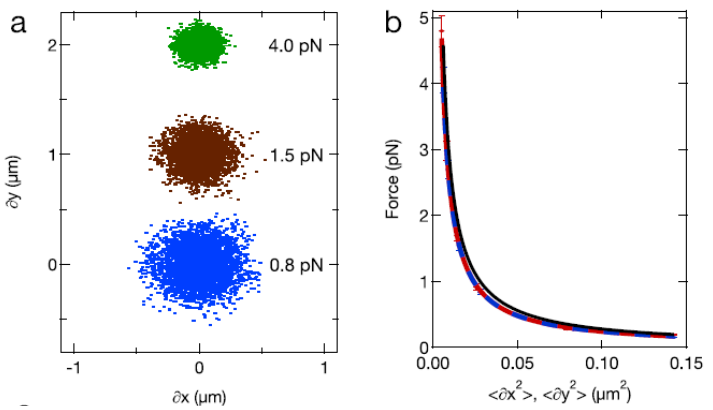

Since the DNA stiffness depends on the applied force, with higher applied magnetic stretching force we expect less movements of the colloid in the x, y direction. This is very similar to a pendulum. In fact this movement can be used to calibrate the forces applied by the magnetic tweezers. The approach is similar to the one we discussed for the optical tweezers, the position histogram will directly reflect the stiffness of the pendulum, allowing to extract the force.

http://www.damtp.cam.ac.uk/user/gold/teaching_biophysicsIII.html

Magnetic Tweezers Forces in x,y

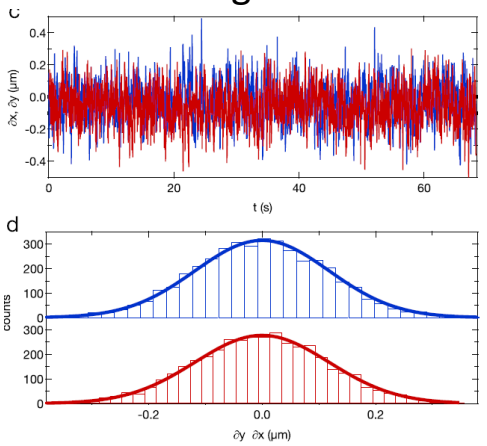

(Koster et al. 2005)

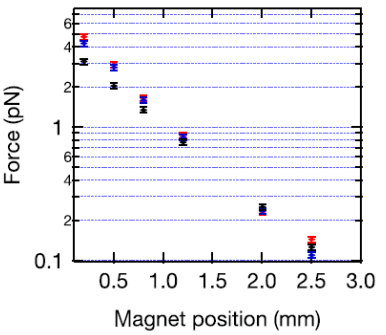

Brownian motion of the magnetic particle reveals the stiffness of the DNA. In real experiments, the fluctuations in x- and y-direction are often not symmetric. This has a variety of reasons, one is that the DNA is not necessarily centrally connected to the particle.
The force on the DNA molecule depends exponentially on the distance of the magnets from the sample. For all practical purposes, the force remains constant if the magnet position is fixed since the gradient is small. This is the reason that magnetic tweezers are force clamps.

http://www.damtp.cam.ac.uk/user/gold/teaching_biophysicsIII.html

Entropic stretching forces

Freely jointed chain (FJC)
(no bending energy)

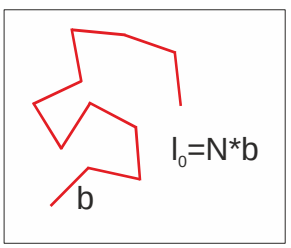

$$z = L\left(\coth\left(\frac{Fb}{k_B T}\right) - \frac{k_B T}{Fb}\right)$$

Worm-like chain (WLC)
(with bending energy)

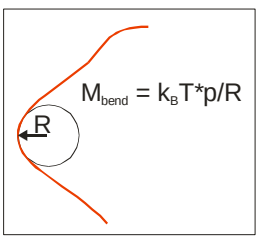

$$F = \frac{k_B T}{p}\left[\frac{1}{4}\left(1 - \frac{z}{L}\right)^{-2} - \frac{1}{4} + \frac{z}{L}\right]$$

http://www.damtp.cam.ac.uk/user/gold/teaching_biophysicsIII.html

Deriving force extension relations

Freely jointed chain (FJC)

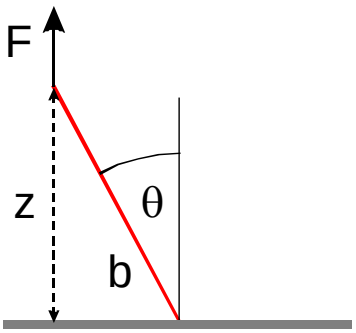

Boltzmann factor

$$U = -Fb\cos\theta$$

$$p(\theta)\cdot d\theta = \frac{1}{Z}\exp\left(-\frac{U(\theta)}{kT}\right)\sin\theta\cdot d\theta$$

$$Z = \int_0^{\pi} p(\theta)\cdot d\theta = \frac{1}{Fb/kT}\left(\exp\left(\frac{Fb}{kT}\right)-\exp\left(-\frac{Fb}{kT}\right)\right)$$

Partition function

$$\langle\cos\theta\rangle = \int_0^{\pi}\cos\theta\cdot p(\theta)\cdot d\theta$$

$$\langle\cos\theta\rangle = \coth\left(\frac{Fb}{kT}\right)-\frac{1}{Fb/kT}$$

Langevin function

$$z = N\cdot b\cdot\langle\cos\theta\rangle = L\cdot\left(\coth\left(\frac{Fb}{kT}\right)-\frac{1}{Fb/kT}\right)$$

http://www.damtp.cam.ac.uk/user/gold/teaching_biophysicsIII.html

Entropic stretching forces

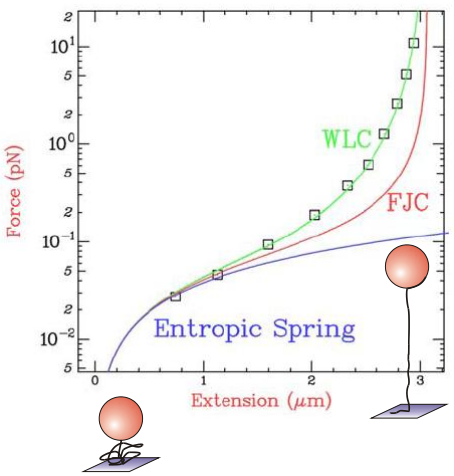

Freely jointed chain (FJC)
(no bending energy)

$$l = l_0\left(\coth\left(\frac{Fb}{k_BT}\right)-\frac{k_BT}{Fb}\right)$$

Worm-like chain (WLC)

$$F = \frac{k_BT}{p}\left[\frac{1}{4}\left(1-\frac{x}{L}\right)^{-2}-\frac{1}{4}+\frac{x}{L}\right]$$

http://www.damtp.cam.ac.uk/user/gold/teaching_biophysicsIII.html

Stretching a single DNA molecule

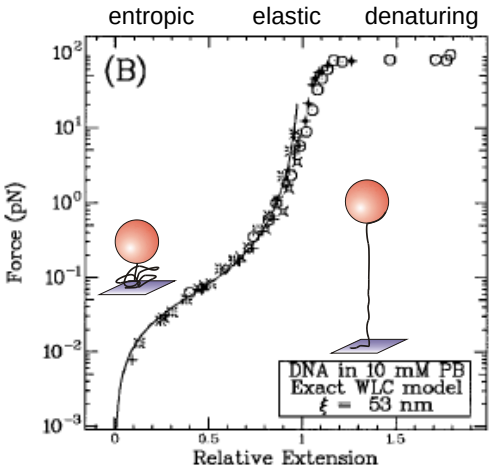

Bensimon et al. 1998

Entropic force component:

WLC model

$$F = \frac{k_B T}{l_p}\left[\frac{1}{4}\left(1-\frac{x}{L}\right)^{-2} - \frac{1}{4} + \frac{x}{L}\right]$$

Bustamante *et al.*, 1994

$l_p = \frac{M_B}{k_B T}$ l_p.. persistence length
M_B.. bending modulus

Elastic stretching:

$$\frac{\Delta L_{\text{contour}}}{L_{\text{contour}}} = \frac{F}{S}$$

S = 1200 pN
(elastic modulus)

http://www.damtp.cam.ac.uk/user/gold/teaching_biophysicsIII.html

dsDNA is a Worm-Like-Chain

(Czerwinski 2007)

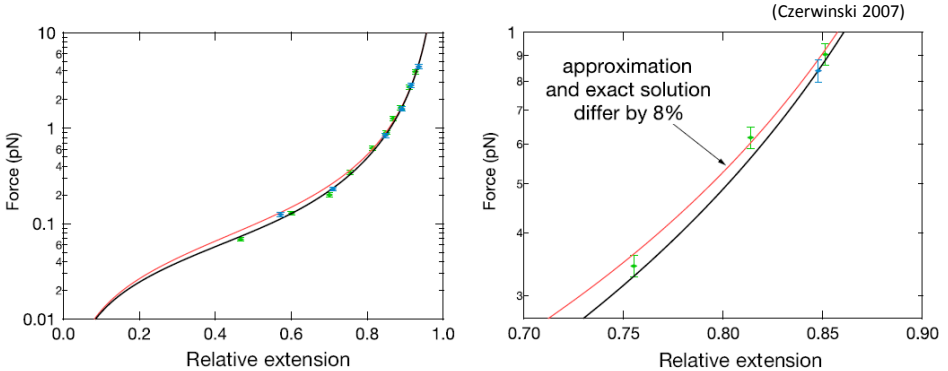

Force extension measured for DNA with contour length L=3.2 µm und 7.0 µm
Red curve: approximated WLC (Marko Siggia)
Black curve: ‚exact' WLC (Croquette et al.)
Difference of up to 8% between 3 pN and 8 pN
(relevant force region for most proteins)

http://www.damtp.cam.ac.uk/user/gold/teaching_biophysicsIII.html

DNA charge important for persistence length

Czerwinski (2007)

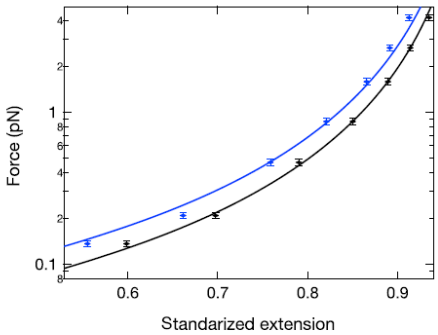

Figure 3.10: Force-extension curves of the same dsDNA molecule in buffer with low salt concentration (monovalent sodium ions $[Na^+]$=1 mM, black data points) and with high salt conditions ($[Na^+]$=50 mM, blue data points) normalized to the contour length L_0 of the DNA molecule. The lines are fits with the exact WLC model yielding values for the persistence lengths of 53 nm (low salt) and 38 nm (high salt). The buffer was TRIS-HCl [50 mM] at pH 7.0.

DNA forms supercoils under Torque

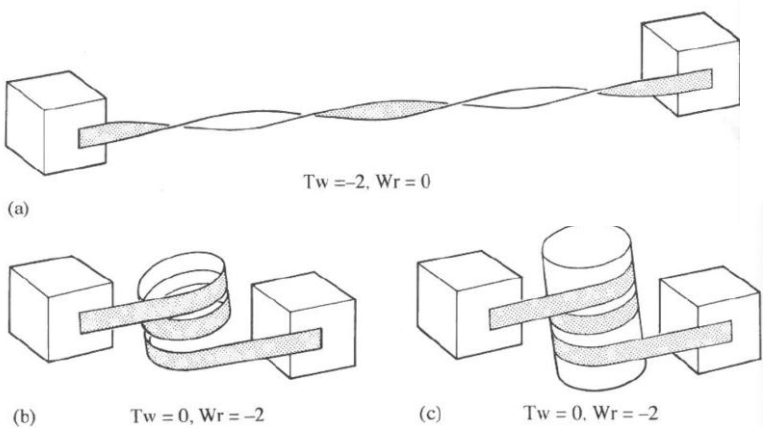

Twisting dsDNA with magnetic tweezers leads to torque on the backbone of the DNA molecule. We can charactersize the state of the DNA with two parameters. The Twist (Tw) and writhe (Wr) describe linking number of DNA $L=Tw+Wr$. The twist denotes the number of helical turns, while writhe counts the number of times DNA crosses itself. Twist can be converted to writhe, when DNA is forming supercoiled structures.

http://www.damtp.cam.ac.uk/user/gold/teaching_biophysicsIII.html

DNA forms supercoils under Torque

Employing magnetic tweezers one is able to study the properties of twisted DNA molecules. Rotating the magnets with the magnetic tweezers leads to torque Γ. The total torsional energy is

$$E=(k_BTC/2L)\theta^2,$$

which is a direct consequence from our treatment with the WLC-model. C is the torsional persistence length and $\theta=2\pi n$ counts the number of turns. We can then calculate the torque to be

$$\Gamma=(k_BTC/L)\theta.$$

At critical torque which is reached at the buckling number n_b, DNA buckles and forms supercoils with radius R as indicated on the right. As soon as the first supercoils formed, the torque remains constant, and additional rotations lead to more supercoils. In other words, for $n>n_b$ energy is stored in plectonemes (writhe) not in twist. As this is done with a force clamp provided by the magnetic tweezers the total energy cost for forming a plectoneme is given by

$$E= 2\pi RF_z + \pi k_BTA/R$$

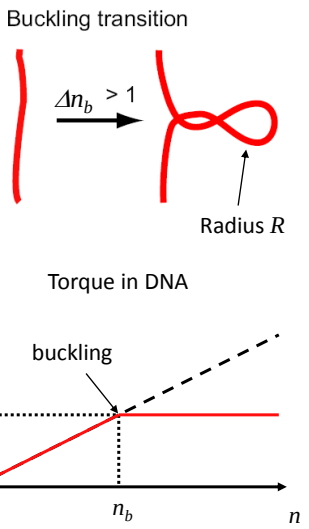

http://www.damtp.cam.ac.uk/user/gold/teaching_biophysicsIII.html

Energetics of supercoiling

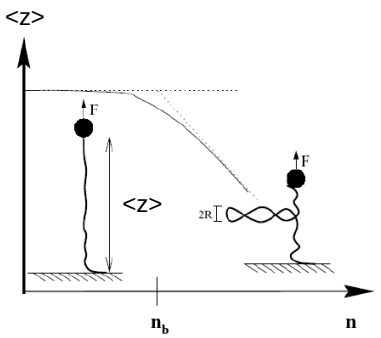

Twisting Plectoneme formation

$$2\pi\,\Gamma_B = 2\pi RF + \frac{\pi k_B T l_p}{R}$$

Work against magnetic force | DNA bending

$\Gamma_B = M_{twist}/\langle z\rangle * 2\pi\, n_B$ …DNA torque

k_BT*l_p ….DNA bending modulus

http://www.damtp.cam.ac.uk/user/gold/teaching_biophysicsIII.html

Magnetic tweezers as torque wrench

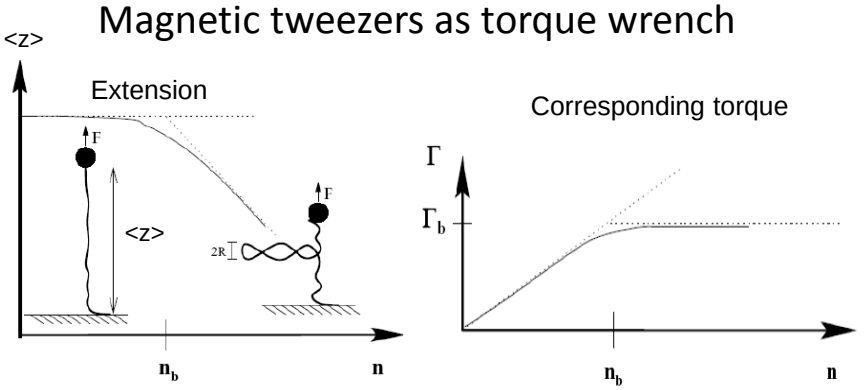

Length change per turn of magnets

$$\Delta\langle z\rangle / turn = \sqrt{\frac{k_B T \cdot l_p}{2F}}$$

Buckling torque

$$\Gamma_B = \sqrt{2k_B T \cdot l_p \cdot F}$$
$$\Gamma_B = M_{twist} / \langle z\rangle \cdot 2\pi N_B$$

http://www.damtp.cam.ac.uk/user/gold/teaching_biophysicsIII.html

Twisting dsDNA at Different Forces

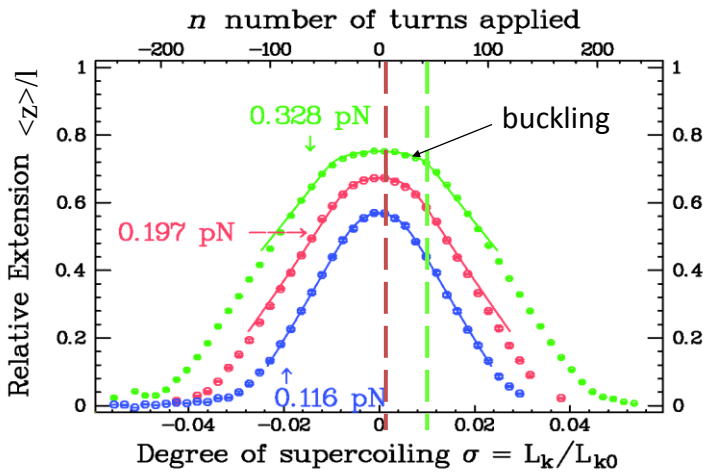

The critical torque for buckling depends on force: hence at higher force one needs to apply more turns before seeing DNA buckling and formation of supercoils. The dashed lines indicate the position when the buckling of the DNA starts. For the lowest force the buckling starts directly.

http://www.damtp.cam.ac.uk/user/gold/teaching_biophysicsIII.html

Structural DNA Transitions due to Torque

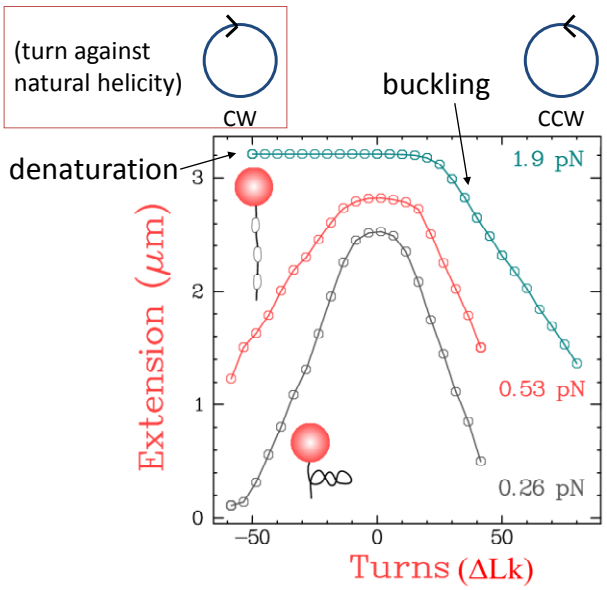

Double-stranded DNA is usually a right handed helix. Twisting the molecule should reveal the asymmetry in the structure. When the DNA is twisted counter clock-wise (CCW) we always observe the formation of supercoils indicated by the shrinking length. However at higher forces, negative turns clock-wise (CW), against the natural helicity, leads to a denaturing of the hydrogen bonds and a total change in the structure. No supercoils can be formed anymore.

http://www.damtp.cam.ac.uk/user/gold/teaching_biophysicsIII.html

Structural DNA Transitions due to Torque

(Allemand et al. 1998)

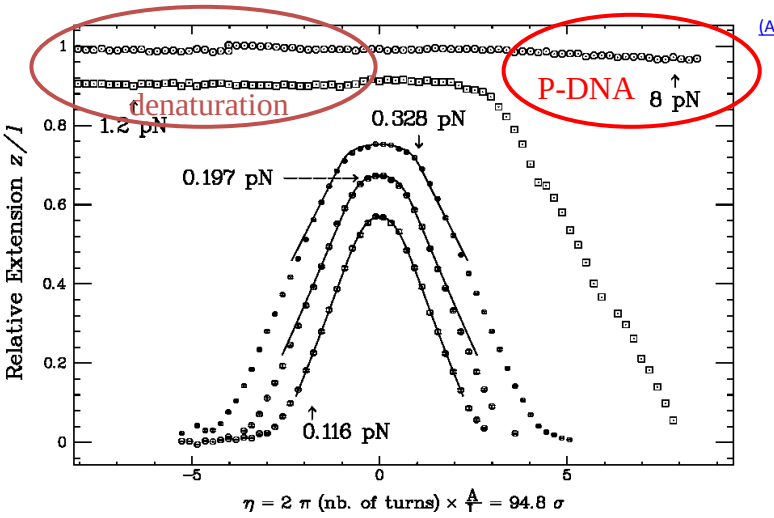

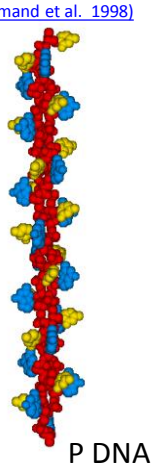

P DNA

At even higher forces, another structural transition of the DNA can seen. At very high stretching the hydrogen bonds denature and P-DNA forms, which is a left-handed helix with the bases turned to the outside. This structure of DNA was proposed by Pauling in the same Nature issue of Watson and Crick's famous paper eraning them the Nobel prize. Of course, the WLC does not include these structural transitions such as denaturation or other DNA forms.

Following a single protein with Magnetic Tweezers

Koster et al. (2005)

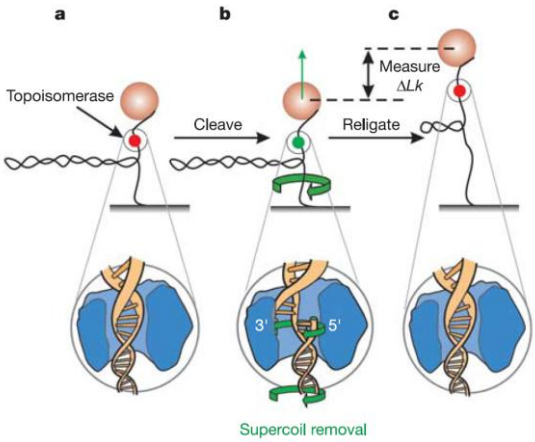

Until now we discussed the magnetic tweezers as instrument to study the structural properties of macro-molecules. However, they can be also used to gather quantitative information on the functions of enzymes that change the state of DNA. One striking example are the topoisomerases which can change the linking number of DNA by cutting one of the backbone strands of DNA. This enables the other strand to rotate in the cavity formed by the protein. The chemical energy to break the bond is stored in the molecule and later used to restore the intact backbone to stop the rotation.

In the following we will see that single protein-DNA interaction can be probed by magnetic tweezers and used to clarify microscopic interactions.

http://www.damtp.cam.ac.uk/user/gold/teaching_biophysicsIII.html

Investigate DNA-enzyme interactions

Koster et al. (2005)

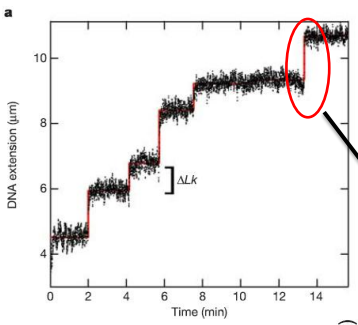

With the magnetic tweezers the linking number of DNA can be chosen by introducing supercoils. When a topoisomerase binds to the DNA, it can change the linking number, indicated by an increase in the distance between the magnetic particle and the surface.

The time resolution of the video detection system allows for studies of the relaxation speed, i.e. how quickly the DNA extension increases for each event. This gives insight about the molecular interactions in the enzyme-DNA system.

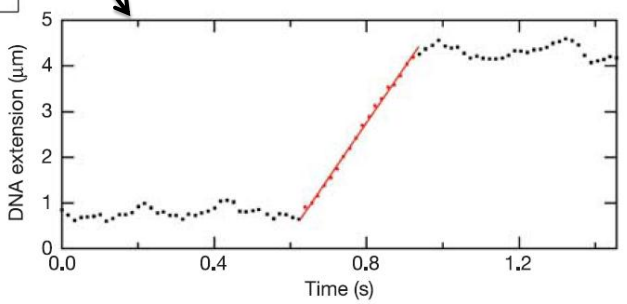

http://www.damtp.cam.ac.uk/user/gold/teaching_biophysicsIII.html

Topoisomerase (TopIB) Removes Supercoils

Koster et al. (2005)

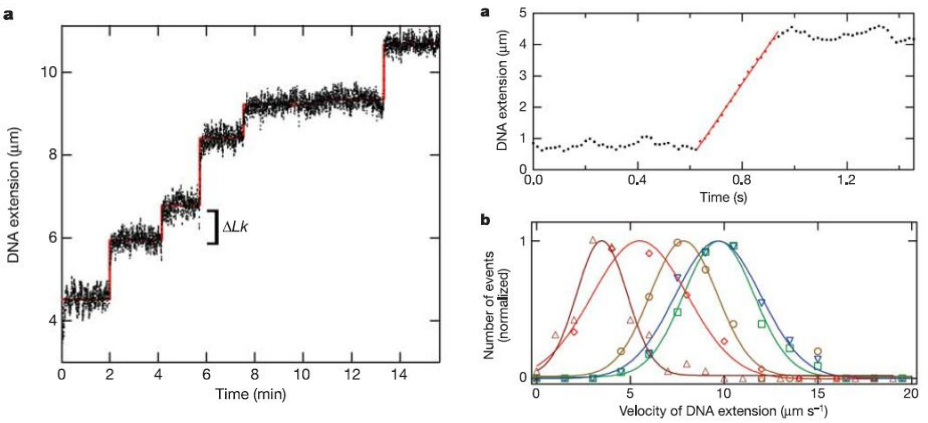

The time resolution of the video detection system allows for studies of the relaxation speed, i.e. how quickly the DNA extension increases for each event. This gives insight about the molecular interactions in the enzyme-DNA system. A single topoisomerase enzyme can remove all supercoils in the DNA molecule. Analysis of the velocity reveals a most probable velocity.

http://www.damtp.cam.ac.uk/user/gold/teaching_biophysicsIII.html

Topoisomerase: friction on molecular level

Koster et al. (2005)

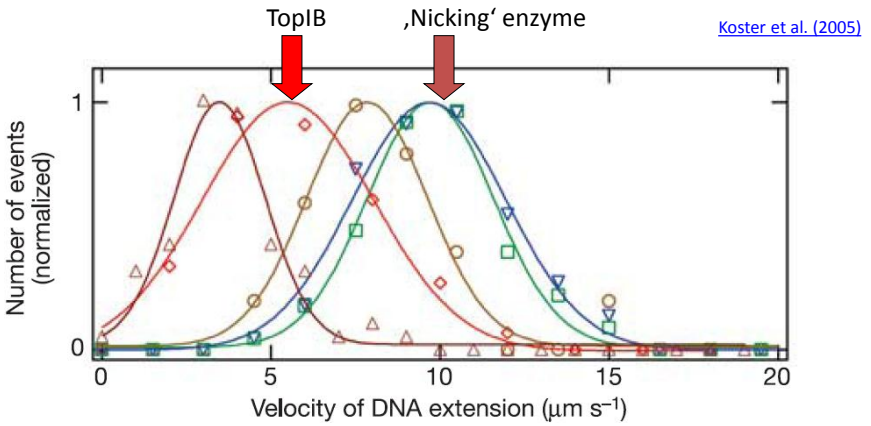

By doing these experiments with a range of different enzymes which perform the same action as the topoisomerase (nicking enzymes create also a double strand break in the DNA) it is possible to prove that the velocity of the DNA relaxation is indeed dominated by the interaction between the DNA and the enzyme. The data shows that for the nicking enzyme the relaxation velocity is almost twice as fast when compared to the topoisomerase enzyme (labelled as TopIB, above). Only conclusion: friction on molecular level slows down relaxation. http://www.damtp.cam.ac.uk/user/gold/teaching_biophysicsIII.html

Interaction between DNA and topoisomerase

Koster et al. (2005)

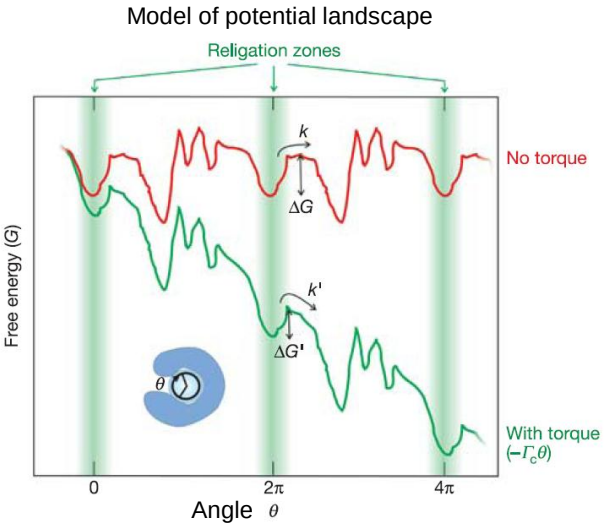

Model energy landscape in protein with several minima

Periodic in 2π

Rate k to cross from one well into the other given by
$k \approx exp(-\Delta G / k_B T)$

Torque Γ applied by MT drives removal of supercoils, assumed to be linear in θ
$k' \approx exp(-(\Delta G - G\, d\theta / k_B T)$

Torque depends on applied stretching force
$\Gamma(F) = (2\, k_B T\, l_p F)^{1/2}$

http://www.damtp.cam.ac.uk/user/gold/teaching_biophysicsIII.html

Force-dependence of step size

Koster et al. (2005)

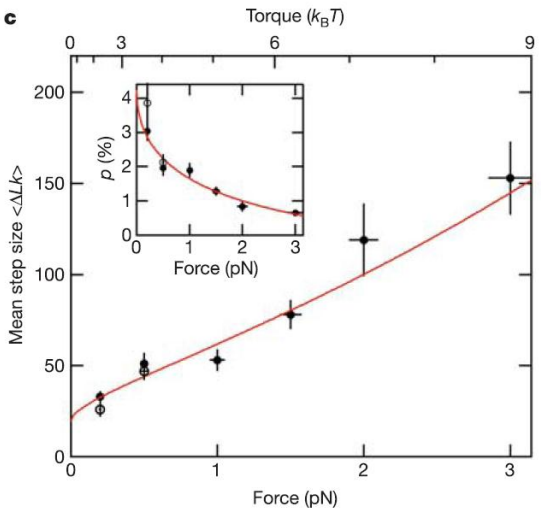

With this simple, qualitative model of the potential landscape we can try to understand the step size in DNA extension curves. As the religation probability p depends now on applied torque Γ:
$p(\Gamma(F))$
In the simplest case we have again a Boltzmann factor depending on the barrier ΔG in the potential landscape:
$p(F) \approx \exp(-\Delta G / k_B T)$
The torque Γ applied by the MT drives removal of supercoils, if we assume this to be linear in θ it follows:
$p(F) \approx \exp(-\Gamma(F)\ \delta\theta\ / k_B T)$
The step size given by the change in linking number ΔLk is now given by:

$$\langle \Delta Lk(F) \rangle = \langle \Delta Lk(F) \rangle_{F=0} \exp\left(\delta\theta \sqrt{2 l_p F / k_B T}\right)$$

The model fits the experimental data very well, strengthening the explanation.

http://www.damtp.cam.ac.uk/user/gold/teaching_biophysicsIII.html

*Topoisomerase (TopIB) as Drug Target **

Koster et al. (2007)

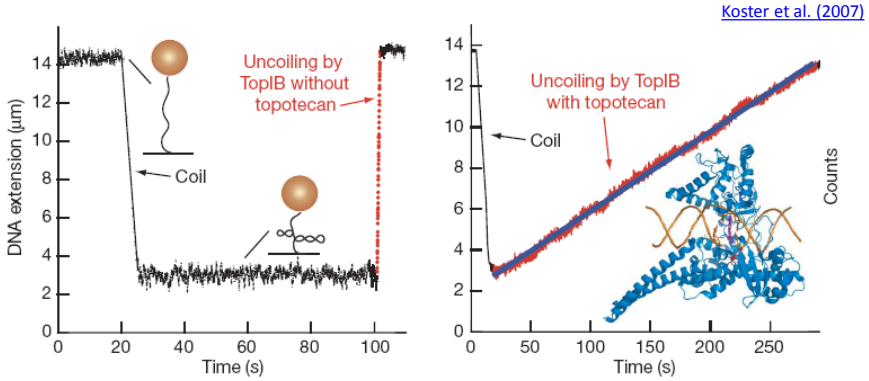

One of the most impressive examples of the potential of single molecule techniques is the clarification of the molecular meachnisms of novel drugs. Topotecan is an important anti-cancer drug which is widely used. However, the exact meachnism was unclear. Magnetic tweezers experiments could show that Topotecon slows down the removal of supercoils by TopIB by several orders of magnitude. This is a direct hint to the biological function can. This is one of the first examples for single molecule techniques helping to clarify drug pathways. Understanding the molecular pathway might guide the future design of imporved drugs.

http://www.damtp.cam.ac.uk/user/gold/teaching_biophysicsIII.html

*Topoisomerase as Drug Target **

(Koster et al. 2007)

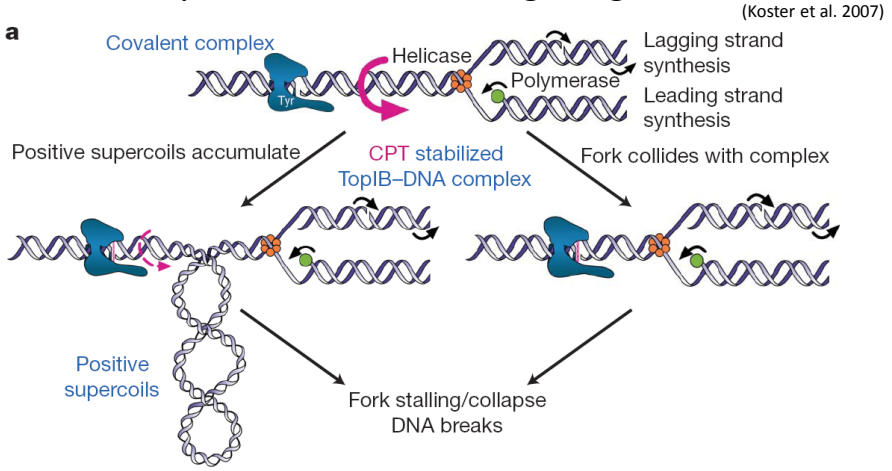

As we saw before, topotecan slows down the removal of supercoils. How does this impede the growth of cancer. For the growth of cancer cells the DNA has to be replicated with an DNA polymerase. This process induces supercoils and thus tension in the DNA molecule beyond the replication fork. The removal of these supercoild by TopIB is slowed down, impeding cancer growth and proliferation.

http://www.damtp.cam.ac.uk/user/gold/teaching_biophysicsIII.html

Primary structure

- 20 typical amino acids side groups for peptide chain, main building blocks of proteins
- Positively or negatively charged (peptides can be polyelectrolytes, separation and manipulation by electric fields possible)
- Side chains (charge, hydrophobicity, polarity) dictate chemical and physical properties of folded protein chains
- Non-standard amino acids are used by bacteria/plants/microorganisms

Table 2.1 The p*K* values for the α-carboxyl, α-amino groups and side chains found in the individual amino acids

Amino acid	pK_1	pK_2	pK_R	Amino acid	pK_1	pK_2	pK_R
Alanine	2.4	9.9	–	Leucine	2.3	9.7	–
Arginine	1.8	9.0	12.5	Lysine	2.2	9.1	10.5
Asparagine	2.1	8.7	–	Methionine	2.1	9.3	–
Aspartic Acid	2.0	9.9	3.9	Phenylalanine	2.2	9.3	–
Cysteine	1.9	10.7	8.4	Proline	2.0	10.6	–
Glutamic Acid	2.1	9.5	4.1	Serine	2.2	9.2	–
Glutamine	2.2	9.1	–	Threonine	2.1	9.1	–
Glycine	2.4	9.8	–	Tyrosine	2.2	9.2	10.5
Histidine	1.8	9.3	6.0	Tryptophan	2.5	9.4	–
Isoleucine	2.3	9.8	–	Valine	2.3	9.7	–

http://www.damtp.cam.ac.uk/user/gold/teaching_biophysicsIII.html

Secondary Structure

(Whitford 2005)

Main structural elements of proteins α-helix and β-strands

Main element is the hydrogen bonds between side chains

http://www.damtp.cam.ac.uk/user/gold/teaching_biophysicsIII.html

α-Helix Protein Secondary structure

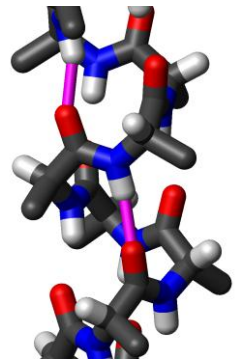

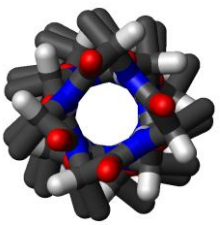

(Whitford 2005)

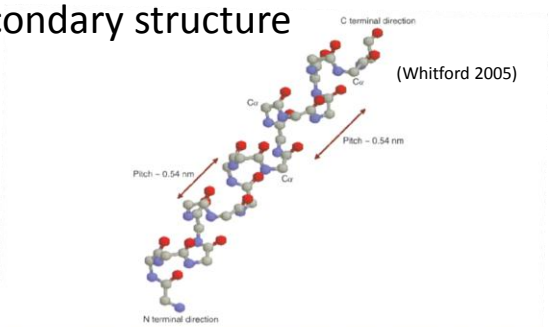

Figure 3.3 A regular α helix. Only heavy atoms (C, N and O, but not hydrogen) are shown and the side chains are omitted for clarity

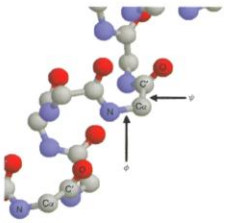

Figure 3.4 φ is defined by the angle between the C′–N–Cα –C′ atoms whilst ψ is defined by the atoms N–Cα –C′–N

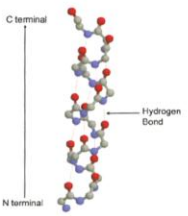

Figure 3.5 Arrangement of backbone hydrogen bonds in a *real* α helix from myoglobin, shows deviations from ideal geometry

Secondary Structure: β-Sheets and Hairpins

(Whitford 2005)

β-hairpin

β-meander

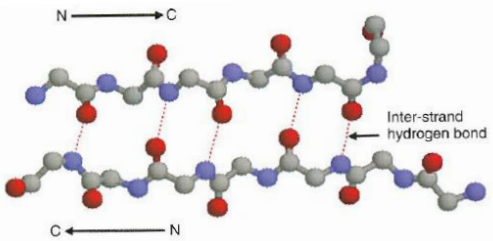

Figure 3.11 Two adjacent β strands are hydrogen bonded to form a small element of β sheet. The hydrogen bonds are inter-strand between neighbouring CO and NH groups. Only the heavy atoms are shown in this diagram for clarity

http://www.damtp.cam.ac.uk/user/gold/teaching_biophysicsIII.html

Protein Tertiary Structure

Example for protein assembly: example movie for beta-barrel

http://www.damtp.cam.ac.uk/user/gold/teaching_biophysicsIII.html

Protein Quaternary Structure

Proteins with several (identical) subunits

mouse cholera antibody

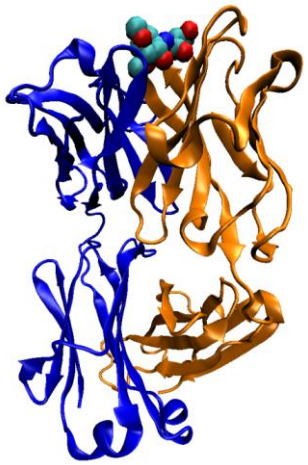

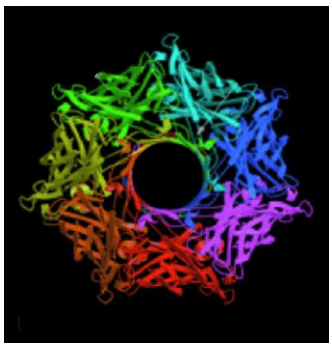

Toxin from
staphylococcus aureus
heptameric 7 identical subunits

http://www.damtp.cam.ac.uk/user/gold/teaching_biophysicsIII.html

Folding Funnel

(Fersht 1999)

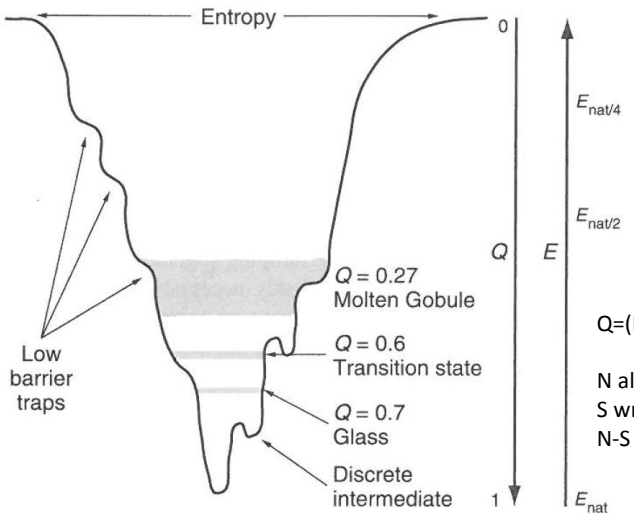

Q=(N-S)/N

N all bonds
S wrong bonds
N-S correct bonds

Figure 19.16 Cross section through a folding funnel. *E* corresponds to free energy.

http://www.damtp.cam.ac.uk/user/gold/teaching_biophysicsIII.html

Folding Funnel for Proteins: Example

(Fersht 1999)

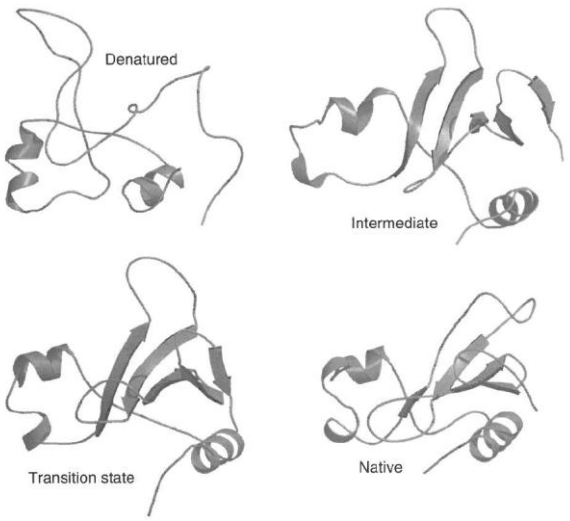

Figure 19.13 Structures of denatured, intermediate, major transition, and native states of barnase from molecular dynamics, Φ values, and NMR. [Coordinates from C. J. Bond, K. B. Wong, J. Clarke, A. R. Fersht, and V. Daggett, *Proc. Natl. Acad. Sci. USA* **94**, 13409 (1997).]

One example for the folding of a protein and representing a nice example for the folding funnel is presented by Barnase. Experimentally, protein folding sub-states of Barnase can be determined with molecular dynamics simulations, magnetic resonance imaging and biochemical analysis. In the ***denatured state*** the protein has two alpha-helices as main structured elements, while in the ***intermediate state*** we can already see the formation of beta-sheets in the protein. The ***transition state*** is already close to the ***native*** conformation of the protein.

http://www.damtp.cam.ac.uk/user/gold/teaching_biophysicsIII.html

Folding Funnel: Connection to Physics

(Fersht 1999)

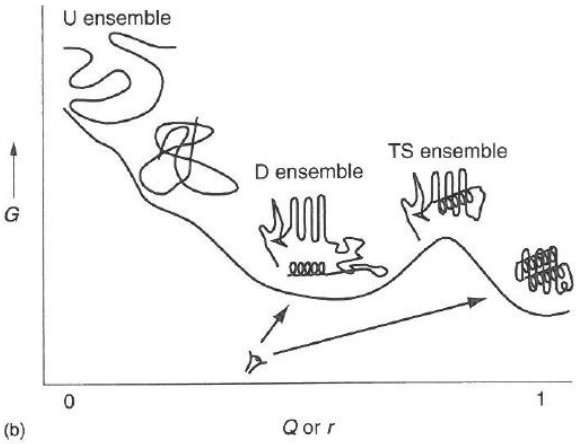

The whole folding process can be rationalized in plotting a free enthalpy G associated to the energy of each of the state as a function of the order parameter Q or reaction coordinate r. In this way it becomes possible to describe the process of protein folding as a succession of barrier crossings which can be formally described with mathematical techniques developed in statistical physics.

Figure 19.17 Reduction of the folding funnel to a conventional reaction coordinate diagram. This reconciles the classical view of a pathway with the new view of an energy landscape and an ensemble of conformations. [After W. A. Eaton, P. A. Thompson, C. K. Chan, S. Hagen, and J. Hofrichter, *Structure* **4**, 1133 (1996).]

http://www.damtp.cam.ac.uk/user/gold/teaching_biophysicsIII.html

Protein Folding

Even small proteins consists of many atoms, and already in the classical description each atom has six degrees of freedom (three for dimensionality, and corresponding three momentum). Considering that proteins are even in solvent (water) with salt ions complicating the situation, protein folding has to be described in a highly dimensional phase space. Just assuming that we have a small protein with 200 atoms has more a phase space with 12,000 dimensions. The interactions lead to the formation of a complex energy landscape for protein folding. Directly related to this there are two main questions for protein folding, how are conformations which a separated by barriers in the energy landscape are crossed by thermally activated processes. The second question is concerned with the overall structure of the energy landscape.

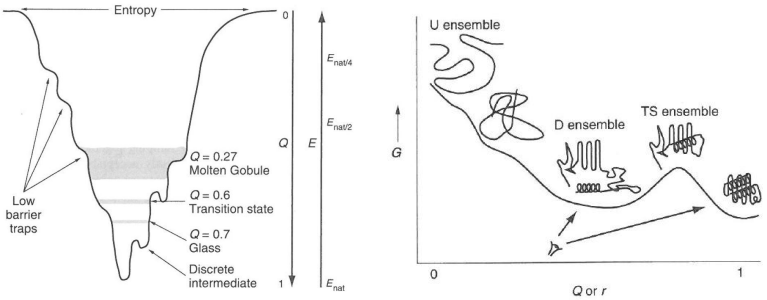

http://www.damtp.cam.ac.uk/user/gold/teaching_biophysicsIII.html

Rate Constants in Protein Folding

Two states (A,B) of the protein should be characterized by a difference in energy ΔG. The rate constant k to change from state A to B can then be given by an Arrhenius type equation:

$$k = \nu_0 \exp(-\Delta G / k_B T)$$

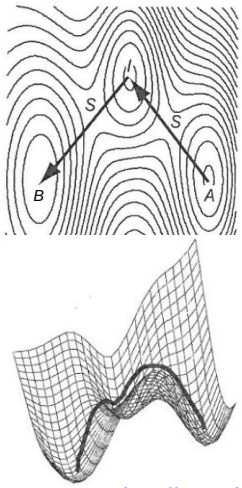

where ΔG is the energy difference between the states and ν_0 is a pre-factor. We will now discuss two approaches to determine ν_0, and at the same time investigate ΔG. A chemical reaction runs along the path with the lowest enthalpy connecting the two states, which was before given in the schematics as the reaction coordinate r. In general the system will try to find the nearest stable minimum in the energy landscape. Since we want to know k we will have to make some assumptions about the exact shape of the energy landscape. This can be illustrated by considering a landscape with two minima which are connected by a saddle point. As soon as the protein reaches a point beyond the saddle point it will end up in state B. For calculating k we will need to know the details of state A and the saddle but not of the final state.

http://www.damtp.cam.ac.uk/user/gold/teaching_biophysicsIII.html

Reaction Rate from Transition State Theory

One approach to get the rates is to assume that all parts of the reaction path can be approximated as parabolas, which means that we can regard all degrees of freedom along the reaction coordinate as harmonic oscillators. The saddle point has the lowest probability to be occupied as the enthalpy is in all other points raising or falling. With the following assumptions:

1) If the systems is past the saddle it will end up in state 2, non-reversible.
2) If the system is in the saddle point (transition state) it can be described classically and is separable from all other coordinates.

The exact calculation will be shown in one of the questions on the questions sheet.

The rate dN/dt of reactions from particles over the barrier can be shown to follow

$$\frac{dN}{dt} = \frac{k_B T}{h} \frac{Z_S}{Z_A} \exp\left(-\frac{E_0}{k_B T}\right)[A] = k[A]$$

Where ZA is the partition function of the starting point A and ZS the partition function of the saddle point. For the calculation of ZS one has to fix the reaction coordinate to S and integrate over all other degrees of freedom.

For the reaction rate for a single molecule we can now write down k

$$k = \frac{k_B T}{h} \frac{Z_S}{Z_A} \exp\left(-\frac{E_0}{k_B T}\right)$$

http://www.damtp.cam.ac.uk/user/gold/teaching_biophysicsIII.html

Reaction Rate from Transition State Theory

There are a few remarks regarding this result:

$$k = \frac{k_B T}{h} \frac{Z_S}{Z_A} \exp\left(-\frac{E_0}{k_B T} \right)$$

1) The separation of the degrees of freedom at the transition point from the rest leads to the fact that Z_S only contains reactions for which S is stable.
2) The rate depends only on the characteristics of the start and transition states.
3) The rate should get faster at higher temperatures, if this is not the case then then this points to a situations where other intermediate states have to be considered.
4) The eauqation assumes that E_0 can be interpreted as the thermal (measured) activation energy. However, this is only a good approximation for small proteins. For larger molecules it is not always possible to separate the degrees of freedom. Then one has to take these effects into account and entropy becomes important. The activation energy is then a free enthalpy.
5) The main result is the pre factor which gives a fundamental rate as
   $k_B T/h$=6.13x10^{12} Hz
   at room temperature which gives a fundamental timescale for chemical reactions in the range of picoseconds.

http://www.damtp.cam.ac.uk/user/gold/teaching_biophysicsIII.html

Kramers Theory for Protein Folding

The transition rate theory does not take into account that the motion in the complex energy landscape is usually overdamped. One obvious reason is that there are so many degrees of freedom in the system that as soon as momentum is transferred from one molecular group to another in the molecule, it is extremely unlikely that this will be transferred back into the reaction pathway. The thermal activated passage over the barrier connecting two states can again be described as the motion of a point in the energy landscape. We will assume that we look at the overdamped case only assuming that at every point along the reaction the system is in equilibrium. This means that we will be able to describe the system in analogy to a diffusion problem.

We will now assume the Gibbs free energy of the system is given by $G(r)$, where r is the reaction coordinate of the system and write down the chemical potential

$$\mu(r) = G(r) + k_B T \ln x(r)$$

With $x(r)$ is the probability density to find the system at position r. Assuming that our particle diffusing in this landscape has a friction coefficient γ, we can write down the average drift velocity as

$$u = -\gamma^{-1} \frac{\partial \mu(r)}{\partial r}$$

http://www.damtp.cam.ac.uk/user/gold/teaching_biophysicsIII.html

Kramers Theory for Protein Folding

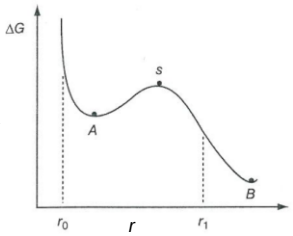

The flux is now given by

$$j = xu$$

and as expected for diffusion problems we have continuity

$$\frac{\partial j}{\partial r} + \frac{\partial x}{\partial t} = 0$$

all equations are already given in one-dimensional form to simplify the system. Combining the three last equation we find that the time development of x can be written as

$$\frac{\partial x}{\partial t} = -\frac{\partial j}{\partial r} = \frac{\partial}{\partial r}\left(\frac{x}{\gamma}\frac{\partial G}{\partial r} + \frac{k_B T}{\gamma}\frac{\partial x}{\partial r} \right)$$

This is also known as the Smoluchowski equation which is the overdamped case of the Fokker-Planck equation. If G is constant along the reaction coordinate then we would get the simple diffusion equation with the diffusion constant $k_B T/\gamma$. With this equation we can now calculate the reaction rate k.

http://www.damtp.cam.ac.uk/user/gold/teaching_biophysicsIII.html

Atomic Force Microscope (AFM)

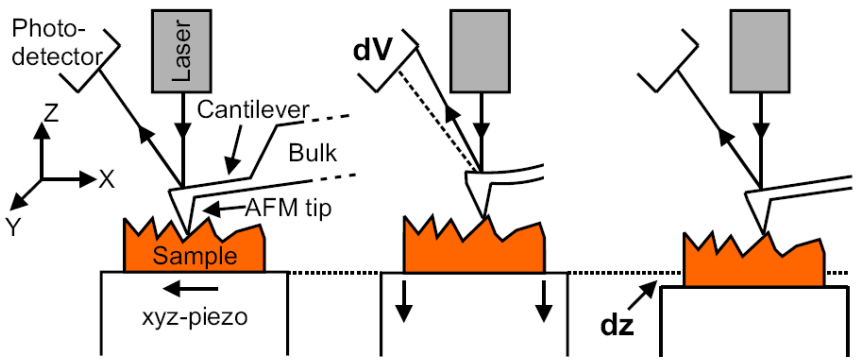

The atomic force microscope consists of three key elements. The imaging system (laser and photodetector), tip for imaging the sample mounted on a cantilever arm and a piezoelectric stage which controls sample position. The force is controlled by detecting the bending of the cantilever arm which can be approximated as a classical spring. The topography of the sample is measured by keeping the photodetector signal (force) as constant as possible. This is achieved by moving the sample with sub-nm accuracy in three dimensions using the piezoelectric stage. Spatial resolution depends on sharpness of tip and force resolution on the total mass of the cantilever.

http://www.damtp.cam.ac.uk/user/gold/teaching_biophysicsIII.html

*Tips for atomic force microscopes **

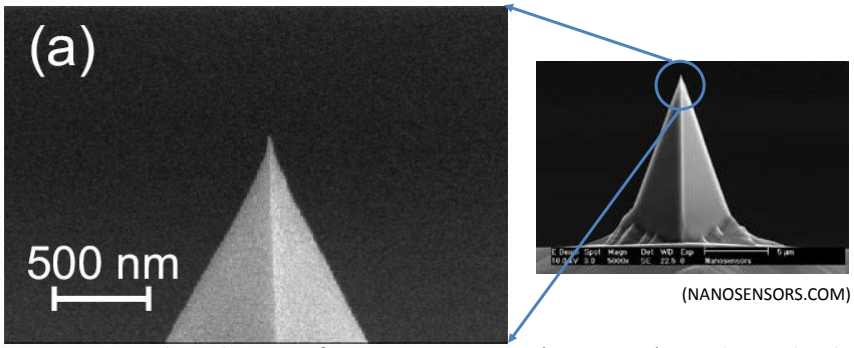

(NANOSENSORS.COM)

The easiest approach to obtain tips for AFM is using a wet (anisotropic) wet-chemical etch of silicon. The etching rates along the different crystal axis is different and leads to a pyramidal tip as shown above with diameters at the sharp end of below 10 nm. With these tips atomic resolution can be achieved. However, there are more sophisticated approaches for making AFM tips, which can now be functionalized with carbon nanotubes to achieve higher resolution, and imaging samples with high aspect ratios (height/width). It is interesting to note that imaging of single atoms even at room temperature is possible. The AFM is Ideally suited for soft (polymers) or biological samples due to possibility to work in liquids especially water.

http://www.damtp.cam.ac.uk/user/gold/teaching_biophysicsIII.html

AFM: Imaging biological membranes and proteins

(Engel 2007)

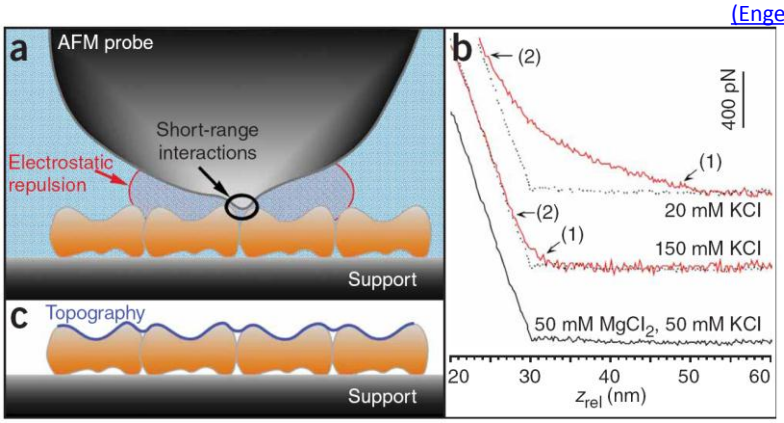

The interactions between tip and sample are critical for the resolution. Taking into account that there are a number of interactions we have to take into account, electrostatic, van der Waals, hydrophobic, etc. this is a complex problem. However, in aqueous solutions containing salt the tip-sample interaction can be tuned by adjusting the salinity and the type of ions in the solution surrounding the sample to minimize long-range interactions and enable a direct contact between AFM tip and sample surface resulting in the highest spatial resolution.

http://www.damtp.cam.ac.uk/user/gold/teaching_biophysicsIII.html

Imaging biological membranes

(Engel 2007)

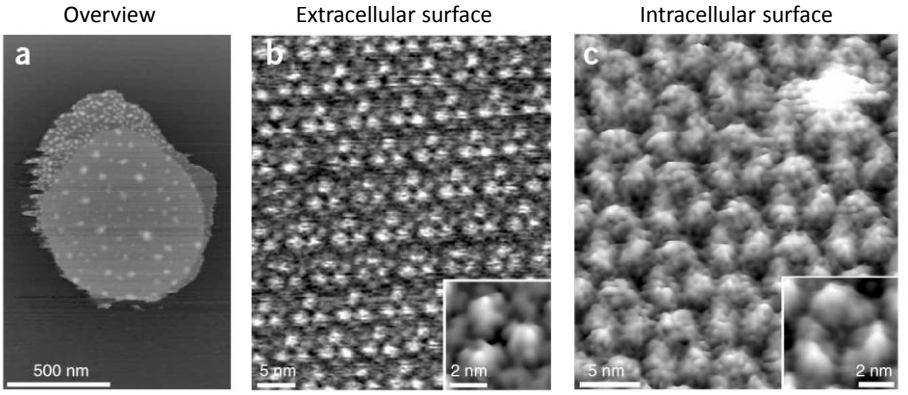

One of the most striking examples for the imaging of membranes and their proteins are the images obtained for bacteriorhodopsin. Bacteriorhodopsin forms a densely packed hexagonal "crystal" in biological membranes. These can be spread out on atomically flat mica surfaces as a support. For the high resolution imaging the aqueous buffer has to be adjusted. To minimize damage to the surface and reduce changes in the proteins the maximum force on the sample is minimized and is around ~100 pN. By overlaying the individual images a high resolution image (insets in middle and right) can be reconstructed.

http://www.damtp.cam.ac.uk/user/gold/teaching_biophysicsIII.html

*Biology: Muscle contraction requires Titin **

Titin (aka connectin) is a protein found in muscles and is responsible for passive tension when muscle is stretched

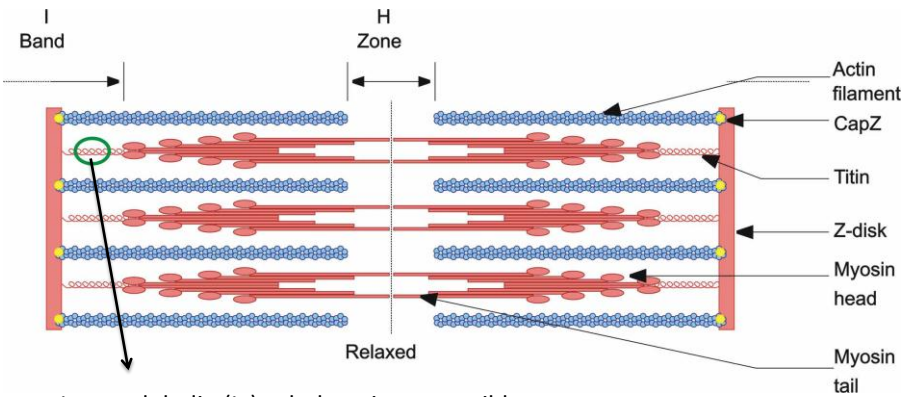

Imunoglobulin (Ig) sub domain responsible for rubber like behaviour of titin

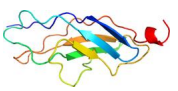

http://www.damtp.cam.ac.uk/user/gold/teaching_biophysicsIII.html

Full Titin 'I-Band' unfolding with AFM

(Gaub 1997)

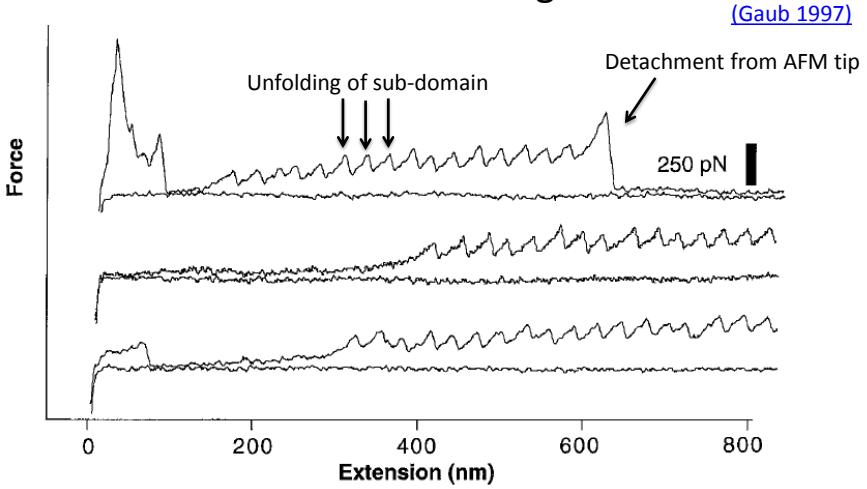

Dynamic force spectroscopy can be used to study the unfolding patterns of proteins. Ig domains of Titin are ideally suited to demonstrate the capabilities of AFM unfolding spectroscopy due to its regular structure with identical sub-domains. Saw tooth pattern in the force-distance plots indicates unfolding of the ingle protein sub-domains in sequential order.

http://www.damtp.cam.ac.uk/user/gold/teaching_biophysicsIII.html

Experimental proof for subunit unfolding

(Gaub 1997)

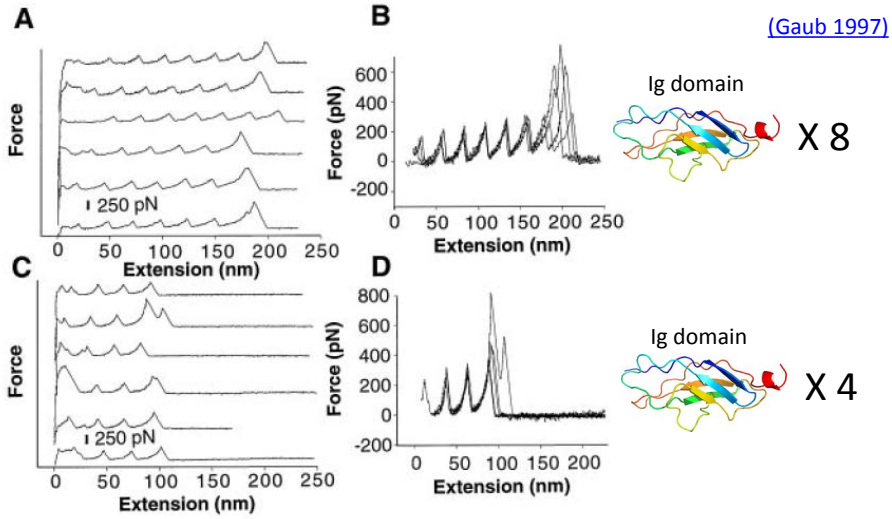

Using biochemical techniques, recombinant Ig domains with a well-defined number of 4 and 8 repeats can be engineered as control experiment. Data fits to expectations perfectly, showing up to 8 unfolding in the upper and up to 4 unfolding peaks in the lower panel.

http://www.damtp.cam.ac.uk/user/gold/teaching_biophysicsIII.html

Refolding of proteins with dynamic force spectroscopy

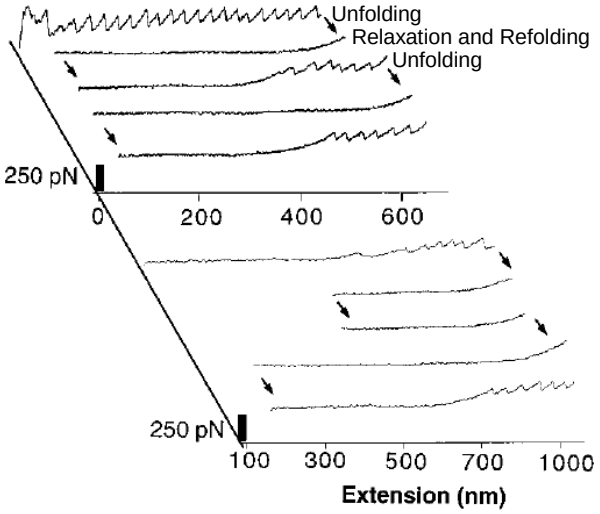

(Gaub 1997)

With the AFM based dynamic force spectroscopy one can also probe the refolding of the domains. Protein refolds only in low force state after the extended chain is relaxed to low extension and thus lower forces. This is an essential proof that the process is reversible and does not induce fundamental changes in the protein. Refolding is force dependent. In high force state no refolding occurs on experimental time scale (lower panel).

Using force spectroscopy with the AFM we can study unfolding and refolding of proteins, the time scales and force dependence of the process.

http://www.damtp.cam.ac.uk/user/gold/teaching_biophysicsIII.html

Unfolding force depends on loading rate

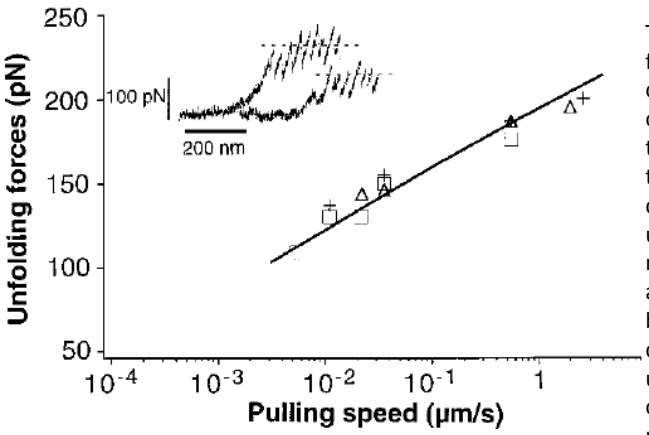

(Gaub 1997)

The maximum unfolding force detected in the process depends on the pulling speed of the AFM retracting from the surface and stretching the protein. We can thus define a loading rate with units of [N/s] which measures how quickly we apply forces to the molecular bonds in the protein. The question is now if we can understand the dependence of the unfolding force on the pulling rate.

This can be understood by simplifying the system into breaking a bond that can either be open or closed. In the next slide we will develop a model for the loading rate dependence using this two-state system.

http://www.damtp.cam.ac.uk/user/gold/teaching_biophysicsIII.html

Unfolding force depends on loading rate

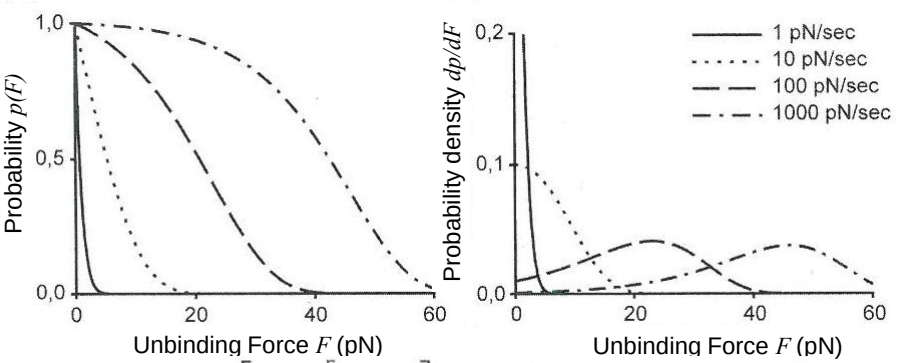

$$p(F) = \exp\left[-\frac{1}{\dot{f}}\int_0^F k_F(\varsigma)d\varsigma\right] = \exp\left[\frac{k_0 F_0}{\dot{f}}\left(1 - \exp\left\{\frac{F}{F_0}\right\}\right)\right]$$

Probability $p(F)$ for a bond to break depends on loading rate $\dot{f}$

With $F(t) = \dot{f}\,t$

http://www.damtp.cam.ac.uk/user/gold/teaching_biophysicsIII.html